

Falling Evaporating Bodies as a Clue to Outline the Structure of the β Pictoris Young Planetary System

Hervé Beust

Laboratoire d'Astrophysique, Observatoire de Grenoble, B.P. 53, F-38041 Grenoble Cedex 9, France
E-mail: beust@obs.ujf-grenoble.fr

and

Alessandro Morbidelli

Observatoire de la Côte d'Azur, Le Mont Gros, B.P. 4229, F-06304 Nice Cedex 4, France

Received September 14, 1998; revised September 27, 1999

Transient redshifted events monitored in the spectrum of β Pictoris have been interpreted for many years as resulting from the evaporation of numerous comet-like bodies in the vicinity of this star. This motivated the investigation of dynamical mechanisms responsible for the origin of these star-grazing comets. Among various ideas, a model involving mean-motion resonances with a jovian-like planet was proposed a few years ago and applied to the β Pictoris case (H. Beust and A. Morbidelli 1996 *Icarus* 120, 358–370). According to this model, the 4:1 and possibly the 3:1 mean-motion resonances are able to generate numerous star-grazers from an initially dynamically cold disk of planetesimals. In this paper, detailed numerical simulations of this dynamical process over a large number of particles are presented, showing in particular that the model is robust toward the presence of additional planets around the star. The question of the evaporation rate of the comet-like bodies is also investigated, showing that, in order to explain the observed spectral events, the comet-like bodies should be larger than 10–20 km, rather than 1 km as previously conjectured. This in turn makes it possible to estimate the typical density of the planetesimal disk required to explain the observed spectral phenomena, i.e., $\sim 10^8$ bodies per astronomical unit in the resonance at 4 AU from the star.

Apart from the main redshifted spectral events, a few blueshifted events were observed over the past few years. These spectral events are clearly distinct from the main redshifted ones and cannot be considered as outliers, although they are far less numerous. In the simple framework of the mean-motion resonance model, these events, which should correspond to bodies moving on differently oriented orbits, should not be expected. We show that assuming the presence of a terrestrial-like planet, well inside the orbit of the jovian planet, may generate these additional events. Close encounters with a terrestrial planet may extract some particles from the resonance, and bring some of them to star-grazing orbits, but with a different orbital orientation, so that they generate blueshifted events.

The question of the refilling of the resonance is investigated. Two basic models may be invoked: First, collisions among planetesimals may replenish the resonance. This appears to be possible, but the mass density of the planetesimal disk in the vicinity of the resonance

needs to be $\sim 10 M_{\oplus}$ per astronomical unit or more, which is hardly realistic. Planetary migration may be a second possible mechanism. A migrating resonance can capture new bodies as it sweeps the disk. We show that this model is realistic only if the migration velocity is high enough, i.e., compatible with models invoking a tidal interaction with the disk, but the reality of this mechanism in the β Pictoris disk must be questioned. © 2000 Academic Press

Key Words: extrasolar planets; planetesimals; celestial mechanics; resonances.

1. INTRODUCTION

The dusty and gaseous disk surrounding the southern star β Pictoris (β Pic), discovered 15 years ago (Smith and Terrile 1984), is regarded today as the leading candidate for an extrasolar young planetary system. Although several planets orbiting other main-sequence stars were discovered in the past years (Mayor and Queloz 1995, Marcy and Butler 1996, Butler and Marcy 1996, Butler *et al.* 1997), β Pic is still a unique example of a young planetary system in its early dynamical evolutionary phase (see recent reviews by Artymowicz 1997, Vidal-Madjar *et al.* 1998).

The age of the star itself is nevertheless still controversial. Paresce (1991) first attributed an age of 2×10^8 yr, attributing its underluminosity to a low metallicity effect. This conclusion was furthermore questioned by Lanz *et al.* (1995). Attributing the underluminosity to extinction, they concluded that β Pic was a truly pre-main-sequence star hardly older than 10^7 yr. Brunini and Benvenuto (1996) and Artymowicz (1997) reinvestigated this question, concluding that on the mere basis of HR diagram comparisons, it was virtually impossible to distinguish between $\sim 10^7$ and $\sim 10^8$ yr, but that the star cannot be much older. Recently the stellar parameters of β Pic have been remeasured by the Hipparcos satellite (Crifo *et al.* 1997), leading in particular to a new estimate of the distance of the star (19.28 ± 0.2 pc) that

was about 18% above the previously commonly assumed values; hence the underluminosity of the star appears now considerably weaker than initially assumed, if existing. Consequently, an age younger than 10^7 yr appears now much less compatible with the data. Moreover, Vidal-Madjar *et al.* (1998) claimed recently that β Pic does not seem to have been in the vicinity of any star-forming region for at least the last 3×10^7 yr. In conclusion, the age of the star very probably lies between 3×10^7 and 1.5×10^8 yr.

β Pictoris definitely appears today as a young main-sequence star close to its ZAMS stage. Its disk cannot thus be a protoplanetary disk characteristic for young stars. This strongly supports models like those of Lecavelier *et al.* (1996) or Artymowicz (1997), describing the disk as a “second generation” structure replenished from inside by larger bodies. The question of the presence of large bodies within the disk appears therefore of crucial interest. In fact, theoretical studies (see, e.g., Lissauer 1993) show that planetary systems are expected to form within a timescale consistent with the age of the star. Although no direct evidence of planets was detected around β Pic as of yet, there are strong indications in favor of the presence of at least one giant (jovian-like) planet orbiting the star: a planet on a slightly eccentric orbit (Lazzaro *et al.* 1994, Roques *et al.* 1994) could generate at least part of the asymmetries observed between the two extensions of the dusty disk (Kalas and Jewitt 1995). Similarly, a planet with a slightly inclined orbit could be responsible for the observed inner warp of the disk (Mouillet *et al.* 1997). Photometric variations have also been claimed as being possibly due to the transit of a jovian planet in front of the stellar disk (Lecavelier *et al.* 1995, 1997a), but Lamers *et al.* (1997) showed that this could alternatively be caused by the transit of a dense dusty cometary cloud.

Surprisingly, the study of the gaseous counterpart of the dust disk also provides clues for the presence of planets. Thank to a favorable edge-on orientation, the gaseous disk was detected spectroscopically (Kondo and Bruhweiler 1985, Vidal-Madjar *et al.* 1986), and it has been the subject of intense investigations since that time. The survey of various spectral lines (Ca II, Mg II, Fe II, etc.) revealed that, apart from a deep central stable component, transient absorption features, usually redshifted, frequently appear or disappear. These additional features evolve within one day or even less (Boggess *et al.* 1991, Vidal-Madjar *et al.* 1994, Lagrange *et al.* 1996, and references therein).

These repeated spectral events have been successfully interpreted as the signature of the evaporation of kilometer-sized bodies in the vicinity of the star, on star-grazing orbits. This model has been termed the Falling Evaporating Body (FEB) scenario. This scenario has been extensively studied in recent years. Dynamical simulations reproduce the observed events in many of their characteristic details (Beust *et al.* 1990, 1996, 1998).

This kind of spectral activity is no longer limited to the β Pic case. Several A-type and Herbig stars exhibit spectral changes or events that are more or less comparable to those observed for

β Pic (Grinin *et al.* 1994, Grady *et al.* 1996, Lecavelier *et al.* 1997b, Cheng *et al.* 1997). In some cases, a FEB-like scenario has been invoked for the concerned stars (Grinin *et al.* 1996, Grady *et al.* 1997).

A key issue concerning the FEB scenario is the identification of a triggering dynamical mechanism capable of putting numerous bodies on star-grazing orbits, out of a Keplerian rotating disk on quasi-circular orbits. Various mechanisms were proposed, all of them involving the gravitational perturbations by at least one planet. These were discussed in Beust and Morbidelli (1996), and the basic conclusions are the following:

- The so-called *Kozai mechanism* concerns orbits initially highly inclined with respect to the orbital plane of a giant planet. Under secular perturbations, these orbits evolve toward low-inclined, but star-grazing orbits (Bailey *et al.* 1992). This is the main source of Sun-grazing comets in the Solar System. Unfortunately, this model has a rotational invariance that predicts an axisymmetrical infall of the FEBs, which is not compatible with the statistics on the available data.

- *Secular resonances* (which require the existence of at least two planets) were invoked by Levison *et al.* (1995) as a possible source for the β Pic FEBs. Indeed, in the Solar System, the ν_6 secular resonance in the asteroid belt is an important source of Sun-grazing asteroids (Farinella *et al.* 1994); the FEBs generated by this dynamical source present dynamical characteristics compatible with the data, in particular a nonaxisymmetric infall. However, invoking the sole action of a secular resonance as a source for FEBs turns out to be a probably nongeneric picture: the strength of the ν_6 resonance is indeed particularly large in the Solar System, due to the specific position and masses of Jupiter and Saturn, and in fact all other secular resonances in the Solar System are much weaker. The same appears very unlikely to occur in other planetary systems, although the additional role of secular resonances in FEB dynamics cannot be excluded (see below).

- *Mean-motion resonances* are also a potential powerful source of star-grazers. More specifically, the 4:1 and, to a less extent, the 3:1 mean-motion resonance with a massive planet on a moderately eccentric orbit ($e' \gtrsim 0.05$) are able to generate numerous FEBs from a rotating disk of planetesimals. The dynamical properties of these FEBs match fairly well those that were deduced from the observation of FEBs toward β Pic. This phenomenon is highly generic, and it is active as soon as one planet is present on a moderately eccentric orbit.

After several years of observations, we have classified the various kinds of spectral events observed in the β Pic spectrum into three distinct sets (Beust *et al.* 1998):

Low velocity features (LVFs) were the first to be identified, being the most frequently observed. They are usually deep (typically 50% of the continuum in various lines), and their redshift velocity with respect to the central component ranges between 10–20 and 50 km s⁻¹. They evolve on timescales on the order of one day, but may be present during several days. This in fact

helped us to estimate their frequency, on the basis of the FEB scenario (Beust *et al.* 1996), leading to a bulk frequency of several hundreds of events per year, with a peak of ~ 8 per day in the periods of highest activity such as December 1992 (Lagrange *et al.* 1996).

High velocity features (HVF) were not immediately identified. They are more distinct and deeper in the UV lines (Al III, Mg II) (Lagrange-Henri *et al.* 1988, 1989). These peculiar elements may reach infall velocities larger than 300 km s^{-1} .

In Ca II lines, components of HVF type were identified somewhat later (Beust *et al.* 1991). Their redshift is typically on the order of 100 km s^{-1} . They are shallower than the HVFs in the UV lines, as their relative depth rarely overcomes 10%, but they are broader than LVFs. They vary very rapidly, within a few hours at most (Lagrange *et al.* 1996). Globally they are less frequent than LVFs. The frequency ratio with respect to LVFs may be roughly estimated to $1/20$ or $1/10$; it must be noted that the higher the redshift, the less frequently the corresponding components seem to occur. Indeed, the most extreme events (above 300 km s^{-1}) have been fairly rarely observed (like in Lagrange-Henri *et al.* 1988), although the corresponding UV lines have been reobserved since that time with HST.

Very low velocity features (VLVFs) were the last ones to be observed (Beust *et al.* 1998). They were identified in Ca II lines, thanks to ultra-high (10^6) spectral resolution, because at lower resolution, they appear blended with the central stable component, their velocities ranging from -10 to $+10 \text{ km s}^{-1}$ with a FWHM of 5 km s^{-1} . The VLVFs are as deep, and even deeper, as the LVFs and may vary on similar timescales. Note also that they verify the correlation noted in Lagrange *et al.* (1996) that makes the width of the variable lines an increasing function of the redshift velocity. Estimating their frequency is even less easy, as they may be detected only with UHRF. However, on the basis of the UHRF data analyzed in Beust *et al.* (1998), we may claim that their frequency is probably at least comparable to that of LVFs if not higher.

In the frame of the FEB scenario, these various kinds of events were successfully interpreted as resulting from different stellar distances of the evaporating bodies when they cross the line of sight (Beust *et al.* 1998): HVFs are due to bodies passing at less than 10 stellar radii (hereafter R_*) ($\simeq 0.08 \text{ AU}$), LVFs to bodies passing (approximately) between 10 and $30 R_*$ ($\simeq 0.24 \text{ AU}$), while VLVFs are due to bodies passing further away, up to the evaporation limit for refractory material ($\sim 0.4 \text{ AU}$). Recall that we are observing variations in metallic lines, and that evaporation of dust is required to generate the observed metallic gas. The various characteristics of the different variable features (velocity, depth, variation timescale, and line width) appear as a natural consequence of the different FEBs distances from the central star. Moreover, it was shown in Beust *et al.* (1998) that the velocity ranges of the three types of spectral events were even better modeled by taking into account the dependence of the FEB's longitude of periastron on the periastron distance, as predicted by the 4:1 mean-motion res-

onance model described in Beust and Morbidelli (1996). Hence the mean-motion resonance model appears reinforced.

The purpose of this paper is first to simulate (Section 2) the mean-motion resonance model, in a numerical way, and compare the results to the observational/modeling statistics of the observed FEBs. We also investigate the crucial question related to the lifetime of FEBs toward evaporation, and we test the robustness of the mean-motion resonance model toward the presence of additional planets. We show afterward in Section 3 that the marginal family of blueshifted LVF-like spectral events recently identified (Crawford *et al.* 1998) is not explained by the model, at least in its simple formulation, but that adding a terrestrial-like planet orbiting the star well inside the orbit of the main jovian planet may account for them. The terrestrial planet extracts some particles from the 4:1 resonance, which subsequently evolve to star-grazing orbit, following a secular—but nonresonant—dynamics. In Section 4, we investigate the question of the refilling mechanism of the resonance, which is necessary if one wants the FEB phenomenon to last over the present age of the star. We show that basically two mechanisms are possible: the resonance may be refilled by collisions or thanks to the migration of the planet. The relevance of both models and their implications concerning the mass of the planetesimal disk are then discussed. Our conclusion is presented in Section 5.

2. TESTING THE MEAN-MOTION RESONANCE MODEL

2.1. A Large-Scale Simulation for the 4:1 Resonance

In Beust and Morbidelli (1996), we analytically showed that the 3:1 and 4:1 mean-motion resonances with a jovian-like planet are possible active sources of FEBs, and we successfully checked our model with numerical integrations of the dynamical evolution of a few test particles. We concluded that the 4:1 mean-motion resonance is expected to be the most powerful source, as almost every particle trapped into this resonance is able to dynamically evolve up to eccentricity $e \simeq 1$, while in the 3:1 case, only those particles having initially $e \gtrsim 0.2\text{--}0.3$ may be subject to such an evolution.

In Beust *et al.* (1998), comparing the evolution of a few test particles to the observational data, we constrained the orbital parameters of the jovian-like planet responsible for the phenomenon. The best fit was achieved with $a' = 10 \text{ AU}$, $e' = 0.07$, and $\varpi' = -70^\circ$ with respect to the line of sight. Here a' is the semi-major axis of the planet, e' its orbital eccentricity, and ϖ' its longitude of periastron. This work gave however no information about the statistical properties of the orbits of FEBs coming from various mean-motion resonances, in terms of both distribution of events velocities and number of expected events.

Obtaining this kind of statistical information requires us to numerically integrate the evolution of a large number of test particles. We thus carry out numerical simulations of 10,000 test particles, initially taken in/close to the 4:1 mean-motion resonance, using the Mixed Variable Symplectic integrator

developed by Levison and Duncan (1994). The planetary orbital data we assume are those listed above. The mass ratio between the planet and the star is assumed to be 0.001 (leading to a planet \sim twice as massive as Jupiter), as in Beust and Morbidelli (1996), but, as noted in that paper, this last parameter is not by itself a very critical one.

The line of sight is assumed for simplicity to lie in the orbital plane of the planet. This choice is guided by the edge-on location of the β Pic disk as viewed from the Earth. However, as noted by Kalas and Jewitt (1995), the actual tilt angle falls probably in the range 2° – 5° . Moreover, there might be an additional inclination angle of the orbit of the planet with respect to the equatorial plane of the disk. That was indeed proposed by Mouillet *et al.* (1997) as a possible origin for the observed inner warp of the dust disk (Burrows *et al.* 1995). Hence a residual tilt angle $\lesssim 10^\circ$ between the line of sight and the orbital plane of the suspected jovian planet cannot be excluded. Hence we also performed the same calculations assuming a nonzero tilt angle. The results appear to be almost identical to those presented below assuming a zero angle; such that we will not present them here.

In the first run, we test the efficiency of the 4:1 resonance. The initial semi-major axes are therefore randomly chosen (with uniform probability function, and this applies for all random choices depicted below) between 3.967 and 3.968 AU, and the initial eccentricities similarly between 0 and 0.1, so that most of them are initially inside the 4:1 resonance. The inclinations are chosen randomly between 0° and 5° . All other orbital angular parameters are randomly determined, so that all possible initial resonant configurations are described. Once a given particle reaches a periastron distance closer than the evaporation distance for refractory material (approximately 0.4 AU; see Beust *et al.* 1998), we check whether its orbit actually crosses the line of sight, and if this is the case, the corresponding spectral FEB event is computed, in terms of stellar distance and projected velocity onto the line of sight.

Figures 1–4 describe the results of this simulation. In Fig. 1, the location of all particles at $t = 150,000$ yr is shown in (a, e) space. We see that roughly $\sim 1/5$ of the initial particles are subject to a FEB-like evolution, while the other particles remain at low eccentricity. This is mainly due to two reasons. First, not all are placed inside the resonance. In order to make this appear clearly, the V-shaped borders of the resonance region in (a, e) space (see Beust and Morbidelli 1996) have been superposed to this plot. Hence the nonresonant particles are located below this region. Second, the efficiency of the FEB-generating mechanisms *inside* the resonance appears to be $\gtrsim 40\%$ after $\sim 10^5$ yr. The efficiency cannot reach 100%, contrary to what could be deduced from the phase portraits displayed in Beust and Morbidelli (1996). The latter were valid for particles having initially a negligible libration amplitude of their resonant motion. Numerical integrations show that if the initial libration is large enough, no FEB-like evolution is obtained. The present simulation nevertheless shows that FEB-like behaviors are fairly common among resonant particles. We recall here that we define a FEB as a body

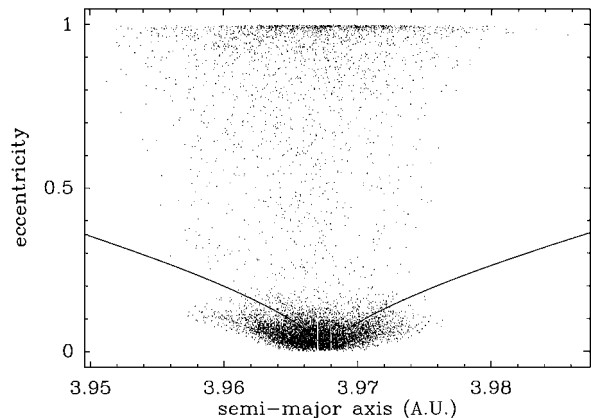


FIG. 1. Result of the integration of 10,000 bodies in the 4:1 resonance. The locations of all particles at $t = 150,000$ yr in a (a, e) space is indicated by dots. The gray rectangle outlined by white lines shows the initial location of the particles. The V-shaped curve denotes the border of the resonant region of the 4:1 resonance. Resonant particles are located above this curve. A clear distinction appears between particles which actually did undergo a FEB-like evolution, and those which did not staying at low eccentricity.

that reaches an high enough eccentricity to allow the periastron distance to enter the dust evaporation zone, i.e., $q \lesssim 0.4$ AU; in the present case, this means $e \gtrsim 0.9$. Such a body is then able to generate spectral events in metallic lines when crossing the line of sight.

As noted in Beust and Morbidelli (1996), the characteristic time for a given particle taken initially at $e \simeq 0$ inside the resonance for becoming a FEB is $\sim 10^4$ planetary revolutions. It may be smaller if the initial eccentricity is significant. This is well illustrated in Fig. 2, where the total number of computed events per year (i.e., the FEB arrival frequency averaged over 1 yr) is plotted as a function of time. The activity clearly becomes high after 10^5 yr. As the orbital period of the assumed planet is ~ 24 yr, we see that this is compatible with 10^4 planetary revolutions or a bit less.

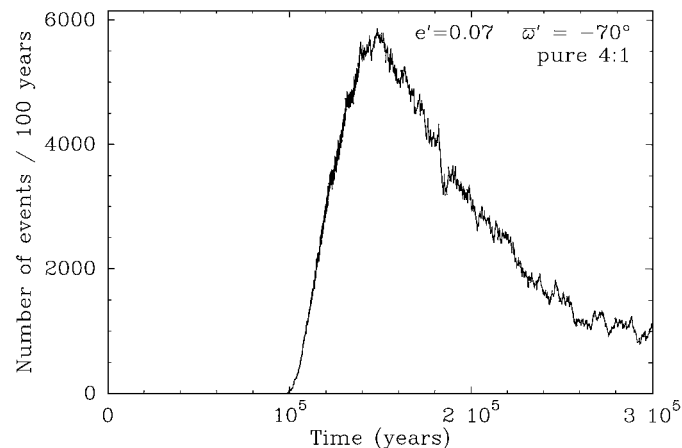


FIG. 2. Histogram of the bulk frequency of FEB-like spectral events as a function of the time elapsed since the beginning of the computation. The activity becomes high after $\sim 10^5$ yr.

This of course raises the question of the refilling mechanism of the resonance. If the characteristic time for a resonant particle to evolve from $e \simeq 0$ to $e \simeq 1$ is typically 10^5 yr, and if it is assumed to be destroyed at that stage, then some mechanism must replenish the resonant region from the disk; otherwise the resonance should be cleared out rapidly and the phenomenon should disappear. This in fact shows up already in Fig. 2, where the events frequency drops toward the end of the run, as a consequence of the absence of any refilling mechanism. In fact, there are some potential mechanisms that could help refilling the resonance, such as collisions among planetesimals, or planetary migration. These are discussed in Section 4.2.

The timescale for clearing out the resonance may in fact depend on the initial conditions that we assumed in our run. Testing different initial eccentricity of inclination distributions, we denote variations that are in any case less than 50%, so that the basic conclusion remains. This timescale also appears to depend on the mass of the perturbing planet. In fact, various tests show that is almost exactly proportional to $1/\mu$, where μ is mass ratio of the two primaries; this may be explained as follows: when the mass of the planet is small compared to that of the star, the topology of the resonant Hamiltonian (i.e., the level curved displayed in Beust and Morbidelli 1996) does not depend very much on the mass of the planet. Besides the perturbing Hamiltonian itself is obviously proportional to μ , and subsequently the same applies to the temporal derivatives of the orbital elements. Hence the characteristic time for exploring the same dynamical evolution is just $\propto 1/\mu$. Now, if we wanted our timescale to be comparable to the age of the star, the planet should be 100 or 1000 times less massive that we assumed. It would thus be a terrestrial planet, but in that case, the width of the resonance would be too small to allow a significant activity. Collective effects also seem not be compatible with FEBs generated by an Earth-sized planet (see below).

Figure 3 shows an interesting fact. It is a detailed enlargement of Fig. 2 over a few years at a typical date. In Beust and Morbidelli (1996), we claimed that the FEB activity due to the resonant process is expected to present a periodic modulation, due to the fact that the resonant particles tend to pass at periastron at specific dates. This is well reproduced in our simulation. As noted in Beust and Morbidelli (1996), this might account for the activity changes over a characteristic timescale of ~ 2 yr that have been observed between successive observational campaigns. However, the observational data are not numerous enough to say whether these activity changes are really periodic, as predicted. Note that in Fig. 3, the temporal period of the modulation is ~ 6 yr, i.e., one-fourth of the orbital period of the planet. From an observational point of view the period of temporal modulation of the FEB activity cannot be determined yet. It should not be shorter than 2 yr, since the latter is the minimal timescale on which some activity changes have been detected. On the other hand, it should not be larger than ~ 15 yr; otherwise 2 yr would be a too short temporal delay for detecting any change. The 2- and 15 yr bounds on the period of modulation of

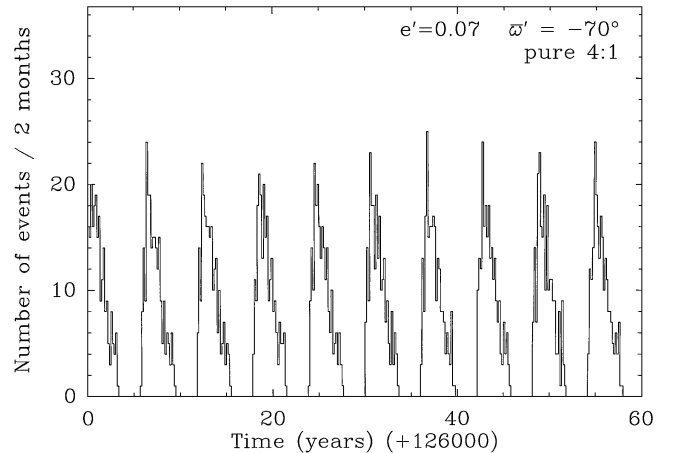


FIG. 3. Same as described in the legend to Fig. 2, but enlarged over a much shorter time span. This makes a sinusoidal-like modulation of the FEB activity over a few years appear. Such a modulation was expected as a consequence of the resonant dynamics (see text).

FEB activity correspond to the planet's semi-major axes equal respectively to 4.8 and ~ 20 AU. Moreover, if the planet is too far from the star, then the mechanism will be much less efficient, as the resonant bodies will have to reach higher eccentricity values to enter the observable FEB regime. We therefore consider 10 AU to be a realistic value for its semi-major axis to be used in our simulations.

Finally, Fig. 4 compares the simulation results with the observational data. Here, for each particle that crosses the line of sight

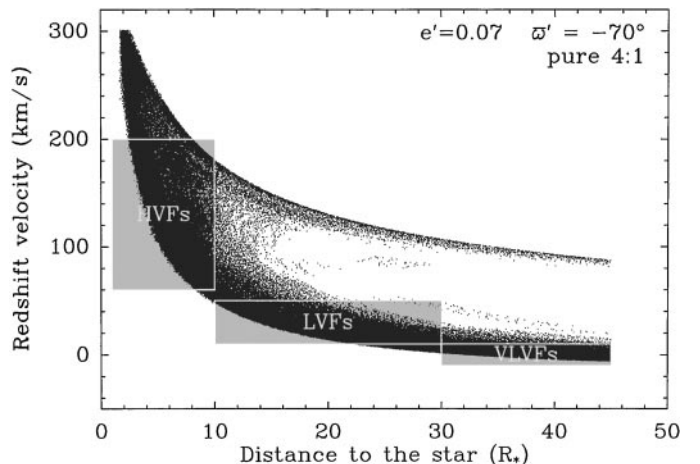


FIG. 4. Plot of the redshift velocity of all computed FEB events, as a function of stellar distance when crossing the line of sight. The gray boxes (outlined with white lines) denote the combined observational/model-dependent constraints on the three different kinds of observed features (HVF, LVF, and VLVF). Note that the borders of these zones are only approximate and somewhat arbitrary. They may be considered accurate to ~ 20 – 30% . The constraint in velocity is of course purely observational, but the distinction in stellar distance between HVFs, LVFs, and VLVs is deduced from our model (Beust *et al.* 1996, 1998).

(i.e., when it generates the spectral event), the observable redshift velocity of the generated variable component is plotted as a function of the stellar distance. As shown in the plot, this may be directly compared to the statistical observational/modeling data concerning the various kinds of variable features observed: the data corresponding to HVFs, LVFs, and VLVs are sketched on the plot as gray boxes outlined with white lines. The fit appears fairly good. In particular, for a given stellar distance, the velocity of the incoming FEBs is constrained within a rather narrow range (this is less true for HVFs), which is in good agreement with the observational data. This is precisely due to the fact that the longitude of periastron of the particles is constrained as a function of the periastron distance by the resonant dynamics. If the longitude of periastron of the incoming FEBs had a random distribution (i.e., an axisymmetrical infall), the dots would spread over a much wider area toward both redshifted and blueshifted velocities. In Fig. 4, the value $\varpi' = -70^\circ$ was fixed in order to achieve the best fit of the observational boxes (Beust *et al.* 1998).

An extra-band of events nevertheless appears in Fig. 4 that does not seem to fit into the observational boxes. This band concerns LVF- or VLVF-like events that would appear at velocities larger than 100 km s^{-1} . Such events were never observed. In fact, we believe these events to be mainly fictitious. The reason is that they all correspond to long-lived bodies that have already passed through their minimum periastron distance following the resonance forced dynamics, i.e., bodies that have already been evaporating for a long time, in any case much longer than for the other bodies. Hence, considering the high evaporation rates needed, most of the corresponding bodies should have fully evaporated before reaching the corresponding zone. This in fact will show up below (Fig. 8) when we will take into account the gradual evaporation of the bodies.

We may conclude that the quantitative numerical simulations confirm the validity of the 4:1 resonance model for the generation of the observed FEBs around β Pic.

2.2. The 3:1 Resonance

As the 3:1 mean-motion resonance is also a potential, but probably less powerful source of FEBs, we perform similar simulations, taking 10,000 particles randomly chosen with semi-major axis in the 3:1 resonance range 4.795–4.82 AU (the 3:1 resonance is larger than the 4:1; see Beust and Morbidelli 1996). The other parameters are the same as before. Figures 5 and 6 illustrate the dynamics inside the 3:1 mean-motion resonance. They must be compared to Figs. 2 and 4. We see that the 3:1 resonance actually generates some events, but is much less efficient than the 4:1 resonance. This is precisely because in the 3:1 case the particles with an initial eccentricity $\lesssim 0.25$ do not normally evolve toward high eccentricity values. Hence a FEB-like evolution in the 3:1 resonance, starting with an eccentricity $\lesssim 0.1$ is the exception rather than the rule. We note also in Fig. 6 that, contrary to the 4:1 case, the particles do not reach the immediate vicinity of the star ($\lesssim 10 R_*$). In other words HVFs are to be expected to appear very rarely from the 3:1 resonance. Forcing the

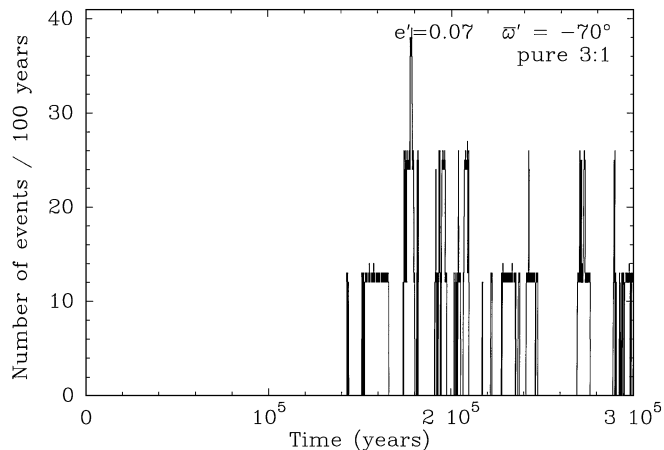


FIG. 5. Same as described in the legend for Fig. 2, but for the 3:1 case. The events frequency is much less than that in the 4:1 case.

3:1 resonance to generate numerous HVFs would require us to assume the semi-major axis of the planet a' to be $\lesssim 2$ AU, which seems less realistic than 10 AU. The bulk velocity range (for a given stellar distance) of the FEBs generated by the 3:1 resonance is identical to that of the 4:1 events, so they could not be distinguished from an observational point of view. For all these reasons we will consider in the following the 3:1 mean-motion resonance as a negligible FEB source compared to the 4:1 one.

2.3. The Gradual Evaporation of Bodies

The numerical simulations presented above have shown that the resonant bodies may become FEBs within 10^5 yr, i.e., less than 10^4 planetary revolutions. In Beust and Morbidelli (1996), we expressed the concern that this delay might be too long compared to the time needed to entirely evaporate a FEB. In fact, the evaporation rates required to produce the observed spectral events are approximately 10^4 times larger than what is reported for Solar System comets ($\sim 10^{29} \text{ molec s}^{-1}$ or $\sim 3 \times 10^3 \text{ kg s}^{-1}$;

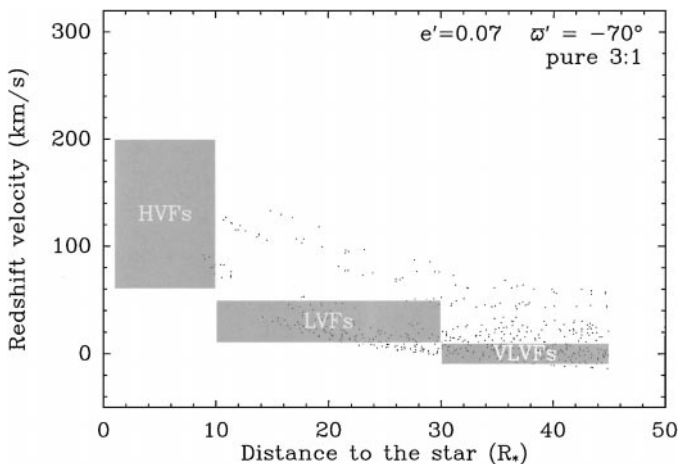


FIG. 6. Same as described in the legend for Fig. 4, but for the 3:1 case. Only a few events are generated, and HVFs are virtually excluded.

see Festou *et al.* 1993), i.e., $\sim 3 \times 10^7 \text{ kg s}^{-1}$ (Beust *et al.* 1996). This high rate should in fact not surprise. It was deduced from LVF observations, i.e., for bodies typically passing at $\sim 0.15 \text{ AU}$ from the star. Hence the FEBs are very close to the star, which is itself approximately 10 times brighter than the Sun (Crifo *et al.* 1997).

The problem is that assuming this evaporation rate, a kilometer-sized body should only resist a few periastron passages before being completely evaporated. Hence the large number of events we accounted in the preceding simulations may appear fictitious, as the corresponding bodies may be fully evaporated far before being able to generate them. This may particularly concern HVFs, as they are generated by the bodies having the closest periastron values, i.e., those which have already undergone the largest number of periastron passages in the evaporation zone before reaching the periastron distance under consideration.

We need therefore to investigate the way rocky/icy bodies may evaporate. Let us first try to model them as comets (this assumption is discussed below). The observation of the FFB phenomenon as spectral variations in metallic lines is related to the evaporation of refractory materials (i.e., dust particles). Hence it only occurs close to the star ($\lesssim 0.4 \text{ AU}$ or $45 R_*$; see Beust *et al.* 1998). However, the activity of a cometary nucleus is expected to start at much larger distances, releasing volatiles and (unevaporated) dust particles. As the dust/gas mass ratio in comets is usually close to 1 (Greenberg 1998), our main parameter is the outgassing rate of the comet-like body. In solar comets, the rate depends highly on the distance to the star, dropping sharply further out than $\sim 4 \text{ AU}$ (see, e.g., recent measurements on Hale-Bopp by Flammer *et al.* 1998). Rickman (1992) introduces a dimensionless empirical function $g(r)$ that gives a convenient fit for the H_2O sublimation flux of an icy nucleus as a function of the heliocentric distance r (in astronomic units), ignoring seasonal effects:

$$g(r) = 0.111262 \left(\frac{r}{2.808} \right)^{-2.15} \left[1 + \left(\frac{r}{2.808} \right)^{5.093} \right]^{-4.6142}. \quad (1)$$

We have of course no coherent model for cometary activity in the vicinity of a star like $\beta \text{ Pic}$, but we will use this law as a first attempt. We apply here a scaling factor in order to set $g(0.15 \text{ AU}) = 3 \times 10^7 \text{ kg s}^{-1}$, i.e., the value required to explain the observed spectral events at a typical stellar distance for LVFs. This leads to an estimate for the mass loss rate $dm/dt(r)$ as

$$\frac{dm}{dt}(r) = \left(\frac{g(r)}{g(0.15 \text{ AU})} \right) \times 3 \times 10^7 \text{ kg s}^{-1}. \quad (2)$$

We are then able to derive the mass loss of the body over a whole orbital period as

$$\Delta m = \frac{P(1 - e^2)^{3/2}}{\pi} \int_0^{2\pi} \frac{dm}{dt}(r(v)) \frac{dv}{1 + e \cos v}, \quad (3)$$

where P stands for the orbital period of the body, e for its orbital eccentricity, and v for the true anomaly along its orbit. We are

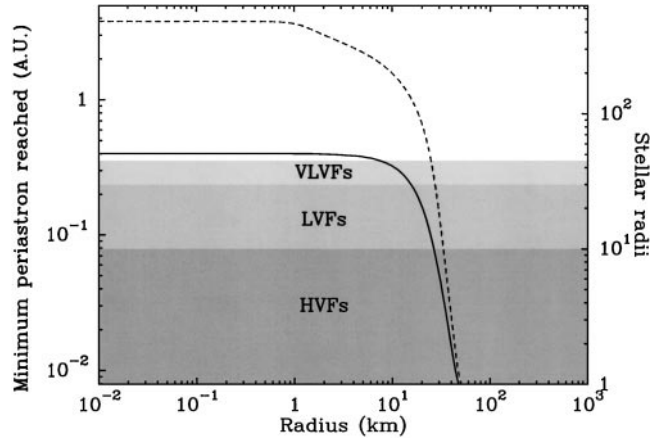


FIG. 7. Minimum periastron reached before complete evaporation for bodies trapped within the 4:1 mean-motion resonance with the assumed jovian-like planet, starting with $e = 0.05$ as a function of the initial radius of the body. The dashed line corresponds to the full use of the evaporation rate of Eq. (1), while the solid line was obtained with the same function, but truncated at 0.4 AU . The gray areas correspond to the various ranges in stellar distances where the corresponding kinds of observable events are generated. In the white area, the particle is too far away from the star to allow the evaporation of refractory material, so that no observable spectral event is to be expected from such a body.

now able to compute how long a given body trapped in the 4:1 mean-motion resonance may survive before being destroyed by outgassing. Hence, for a typical dynamical evolution simulated before, we compute following Eq. (3) the mass loss for each orbital period, and check how long a body with a given initial radius may resist. This in turns gives the minimal periastron distance that the body may reach. In these computations, we assume the density to be equal to 1 g cm^{-3} .

The results in illustrated in Fig. 7, which plots the minimum periastron reached in the evolution, as a function of the initial radius. The dashed line corresponds to the outgassing rate described by Eq.(1). We see that bodies smaller than $\sim 30 \text{ km}$ radius should not even survive long enough to enter the zone of observable spectral events. HVFs should be expected only from bodies larger than $\sim 50 \text{ km}$.

However, we believe that this extreme picture does probably not match the reality. We must note first that the model we are discussing is in fact a very crude estimate of the secular activity of a comet. It is in fact well known for solar comets that while outgassing water, a comet releases dust grains, and that some of the grains (namely the larger ones) remain at the surface of the nucleus, leading to the formation of a refractory mantle at the surface of the comet (see, e.g., Festou *et al.* 1993), with the consequence of a sharp drop in the outgassing activity, and subsequently to a longer lifetime. This is indeed the model that is frequently assumed for evolved cometary nuclei (Sekania 1991, Flammer *et al.* 1998). This remains however valid as long as the refractory mantle does not itself evaporate, i.e., as long as we are not in the FEB regime.

In order to investigate this scenario, we computed another extreme picture, now assuming that the outgassing activity is

prevented as long as the refractory material constituting the mantle does not evaporate. In practice, we now assume the same outgassing rate law as in Eq.(1), but truncated at stellar distances larger than 0.4 AU. The result is illustrated by the solid curve of Fig. 7. We see that smaller bodies are now able to enter the observable FEB area before being fully evaporated. Note however that, even in this case, 1-km-sized bodies do not resist long enough to reach small periastron distances (they only generate VLVFs), and that 10-km-sized bodies hardly achieve this. Bodies larger than ~ 30 km are not very sensitive to the shielding effect of the presence of a crust, so that the solid and the dash curves almost coincide for a radius larger than 30 km.

There is also another reason why we think the last truncated evaporation model to be more realistic. Our bodies are assumed to originate from the 4:1 mean-motion resonance with the planet, i.e., ~ 4 AU from β Pic, which is itself an A-type star. Hence, modeling them as comets may appear unrealistic. Indeed, our FEBs are much more likely asteroid-like bodies rather than pure comet-like bodies. Note however that we have no idea about where these bodies did *form*, as the resonance must be continuously replenished with new bodies which may probably be taken in the vicinity, but that may also have formed in a significantly different area. This means that our FEB progenitors may be made of a mixture of dust and ices, but that they should present in any case a refractory surface mantle that prevents the ice from free sublimation. Hence we are back to the idea that the activity of these bodies should be very low until they reach the FEB zone. Their lifetime against evaporation should not be a function of their past dynamical history before entering the FEB regime, but may rather depend on their activity during the FEB phase, i.e., the situation depicted by the solid line of Fig. 7.

The reality is then probably closer to that last picture. Although one should not forget that the present description is very crude. For instance, tidal and/or outburst effects, which probably disrupt individual bodies into several pieces when getting sufficiently close to the star, are ignored. Our computation seems however to imply that the FEB phenomenon could hardly be explained with a population of ~ 1 -km-sized bodies, while a population of bodies mainly larger than 10 km would be better suited. In reality there is probably a wide size spectrum in the FEB population, but small bodies probably do not survive long enough to become observable, while larger ones do. The largest bodies (radius $\gtrsim 40$ km) among this population should be expected to resist down to genuine star-grazing orbits, leading to the most extreme HVFs that are sometimes observed.

2.4. Revising the Simulation

This size spectrum selection effect was not taken into account in the simulation outputs displayed in Figs. 4 and 6, as these simulation were purely dynamical. We thus expect the events to be less numerous than accounted for in those figures, especially in the HVF regime, as most bodies should not survive down to small periastron distance values. We thus introduce the evaporation model illustrated above in the dynamical simulation.

Each of the 10,000 test particles computed is assigned a radius r , randomly chosen following a classical $r^{-3.5}$ differential size distribution

$$p(r) dr = 2.5 \left(\frac{r}{r_{\min}} \right)^{-3.5} \frac{dr}{r_{\min}} \quad (r > r_{\min}). \quad (4)$$

with a given minimal radius r_{\min} . Note that following this distribution, 82% of the bodies verify $r_{\min} < r < 2r_{\min}$ (the mean radius is $5/3r_{\min}$). Hence r_{\min} may be regarded not only as the minimum radius, but also as the typical radius of the particles.

At each timestep, the amount of mass lost by each particle is computed, following Eq. (3) and assuming that the outgassing is truncated at 0.4 AU. Whenever the integrated mass loss reaches the initial mass, the particle is removed from the simulation.

In the case where $r_{\min} = 1$ km is assumed, almost no FEB event is produced, as most bodies evaporate almost instantaneously. Conversely, assuming $r_{\min} = 15$ km leads to a result in terms of number of FEB events generated (Fig. 8) that should be considered as realistic. Comparing to Fig. 4, we note that many fewer events are present, especially in the HVF domain. We see also that the remaining events concentrate in a velocity band narrower than that in Fig. 4. In Fig. 9, we compare the relative importance of the different families of variable events, in order to make direct comparison with the observational statistics given in the Introduction (and in earlier papers such as Beust *et al.* 1998). LVFs and VLVFs appear indeed to dominate the distribution, while VLVFs concentrate into a very narrow velocity range. As expected, the ratio between HVFs and LVFs is small, and perhaps somewhat too small. This ratio depends in fact highly on the evaporation model assumed, which is still rather crude. If we do not take into account the evaporation (i.e., if we consider the situation depicted in Fig. 4), it jumps up to

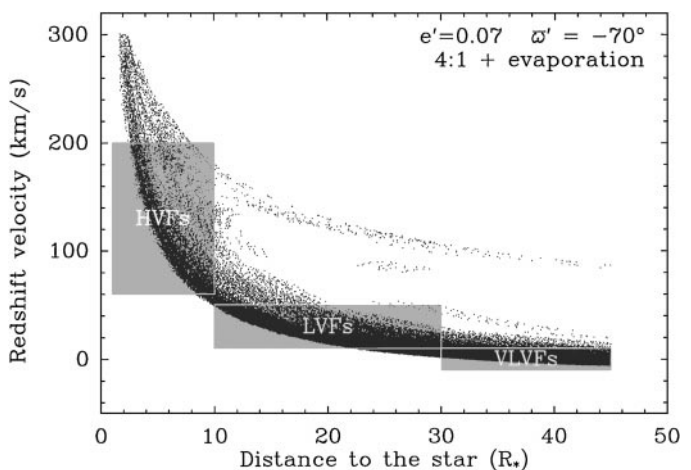


FIG. 8. Same as described in the legend to Fig. 4, but now the gradual evaporation of the bodies was taken into account. The minimum radius r_{\min} was set to 15 km, and the outgassing profile was truncated for distances larger than 0.4 AU. The events appear less numerous, particularly for the HVFs, and they concentrate into a narrower velocity band.

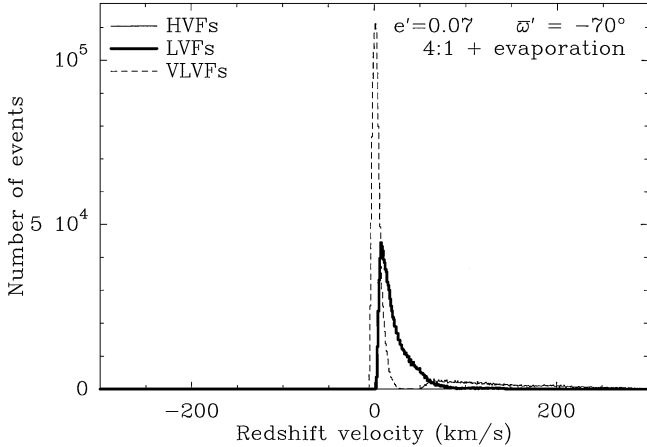


FIG. 9. Under the same conditions as described in the legend for Fig. 8, this plot shows histograms of the predicted velocity distributions for the three major families of variable spectral features. The relative populations and the corresponding velocities must be compared to the basic observational statistics listed in the Introduction.

$\sim 1/4$ or more, and all we can say here is that taking evaporation into account seems to be necessary to better match the observations.

We also see in Fig. 8 that with respect to Fig. 4, the high-velocity LVF-like events, i.e., those corresponding to distances from the star exceeding $10 R_*$ and velocities larger than $\sim 100 \text{ km s}^{-1}$, have almost disappeared. As explained above, this was expected, as the corresponding bodies have usually already fully evaporated before reaching this zone. Even if some of these events still survive in Fig. 8, we see in Fig. 9 that their contribution to the statistics of LVFs is negligible. We cannot however ever exclude an event observed as a high-velocity LVF-like feature, but the fact that none as of yet were detected remains consistent with the predictions.

The present modeling of the evaporation process is of course still very crude, and we will reinvestigate it in more details in future work. Nevertheless we believe that taking it into account leads to a picture more realistic than that obtained by the pure dynamical simulations. Hence, in the following we will always include the evaporation model in the simulations.

2.5. The Planetesimal Population of the Resonance

The present simulations make it possible to estimate the total population of bodies within the resonance. Figures 2 and 3 show that the peak (i.e., the steady-state regime expected) average rate of events is about ~ 60 events/year per 10^4 particles. If we take into account the evaporation, this reduces to ~ 30 events/year. Now, the statistics of the observations reveal that the actual number of observable (not necessarily observed!) FEB spectral events on β Pic is as high as several hundreds per year, with a peak of ~ 3000 or more (8 per day) in the period of highest activity. We may thus estimate the 4:1 resonance to be actually ~ 20 – 50 times more crowded than in our simula-

tion. The actual population in the resonance may be estimated between $\sim 2 \times 10^5$ and 5×10^5 bodies, or a local linear density of planetesimals between $\sim 3 \times 10^7$ and $\sim 10^8$ bodies per astronomical unit. The latter result depends actually on the mass that we assume for the planet, as this parameter affects the width of the V-shaped resonant region in (a, e) space (Beust and Morbidelli 1996). This dependence is nevertheless not very strong, as the width of the resonance scales as the square root of the mass of the planet. Hence, assuming a 10 times less massive planet than initially assumed (i.e., a planet less massive than Saturn) would only require to increase the needed population by a factor 3. Taking into account the uncertainty on the planetary mass (we only assume it is a jovian-like planet), we may safely estimate the local density as between 2×10^7 and 2×10^8 bodies per astronomical unit, values around 10^8 per astronomical unit being the most probable. This is comparable (once scaled to larger stellar distances) to the 10^7 – 10^8 slowly evaporating bodies (orbiting evaporating bodies; see Lecavelier *et al.* 1996) estimated to exist over a ~ 20 AU-wide region in the outer system by Lecavelier (1998), to account for the CO replenishing rate of the disk. Note that this only concerns the population *within* the resonance.

This estimate was made on the basis of the simulation displayed in Fig. 8, where we had assumed initial eccentricities between 0 and 0.1 for our test particles. The efficiency of the FEB mechanism depends however on the initial eccentricity of the particle. A particle having an initially larger eccentricity will undergo an eccentricity pumping effect much more easily. This is why we tested two other situations, one with $0 \leq e_{\text{initial}} \leq 0.05$ and another with $0 \leq e_{\text{initial}} \leq 0.3$. In each case, we scale the initial semi-major axis distribution in order to match the corresponding width of the resonance.

In the first case ($e \leq 0.05$), the results are comparable to those for $e \leq 0.1$ (plots very similar to Figs. 4 and 8 are obtained), but the peak events frequency is now only 10 events per year. Comparing to the observed FEB frequency, this leads to a population estimate between 1.2×10^6 and 3×10^6 bodies in the resonance. Taking into account that the width of the resonance is now only ~ 0.002 AU, the local density estimate turns out to lie between 4×10^8 and 4×10^9 per astronomical unit.

Obviously, assuming a lower initial eccentricity limit would lead to an even higher estimate. However, independently from the fact that this is already a high density, we do not think this to be realistic. Indeed, in the $e \leq 0.05$ run, the *nonresonant* bodies located outside the resonance appear to have reached, under nonresonant perturbations, eccentricities ranging between 0 and ~ 0.1 at the end of the simulations (3×10^5 yr). The same applies also for the $e \leq 0.1$ case. Hence the “natural” eccentricity dispersion of the disk in the vicinity of the resonance appears to be roughly 0.1, so that the corresponding run should be considered as the most probable, keeping in mind that other sources of perturbations (additional planets, secular resonances, etc.) will all tend to possibly increase this limit. This is the reason why we have first presented the results for $e \leq 0.1$.

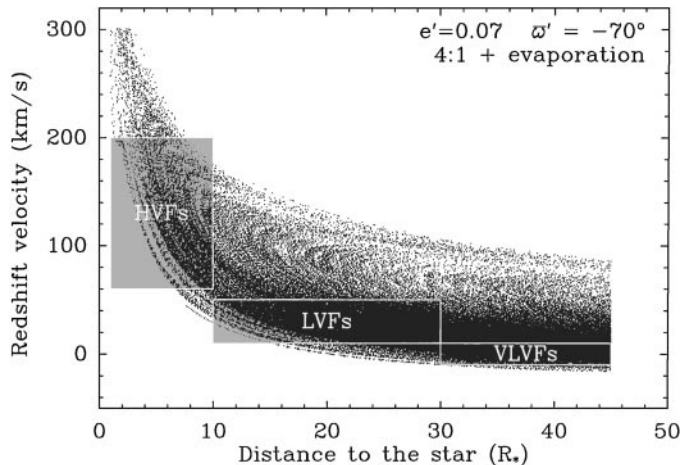


FIG. 10. Same as described in the legend to Fig. 8, but now for initial eccentricities between 0 and 0.3. The fit of the observational boxes is much worse, but taking into account the statistical uncertainties, it could still be considered as acceptable.

Alternatively, we tested also a high eccentricity case, namely $0 \leq e_{\text{initial}} \leq 0.3$. That choice was guided by the present dynamical status of the asteroid belt, and also by the fact that we wanted to test the worst possible case in terms of velocity confinement for the FEB event velocities. In fact, Fig. 10 shows that even in that case, an acceptable velocity confinement is obtained. The fit of Fig. 8 appears however much more satisfactory. Conversely, the peak events frequency reaches now 120 events per year. In terms of density estimates, the requirement is now only $2 \times 10^6 - 2 \times 10^7$ bodies per astronomical unit.

It is in fact thought that the present eccentricity distribution within the asteroid belt was not initial, but rather due to the dynamical sculpting by planetary perturbations (resonant or not) over the entire age of the Solar System. The eccentricity dispersion within the initial asteroid belt should then be less. Hence assuming a eccentricity dispersion among our test particles such as the one we assumed initially ($e \leq 0.1$) could indeed appear more realistic.

2.6. Other Planets. The Robustness of the Model

An important issue concerning the resonant mechanism proposed as a source of FEBs is its robustness. All the calculations presented above fit into the frame of the restricted 3-body problem, i.e., a negligible mass particle perturbed by primaries orbiting on a stable orbit. This is strictly valid if only one planet is present, but in the more realistic situation of a hypothetical complete planetary system, the validity of the above results may be questioned. In other words, we need to test the robustness of the model toward the presence of other planets in the disk.

Of course, as we do not know anything about the hypothetical planetary system of β Pic, we cannot explore all possible planetary configurations. In any case, a strong distinction should be made between *outer* and *inner* planets with respect to the main one. It is obvious that an inner planet, i.e., orbiting the star inside the location of the jovian resonance, has a potentially much

more powerful disturbing effect on the FEB mechanism. Indeed, whenever the resonant bodies reach large eccentricity values, they must cross the orbit of the inner planet, with the possible consequence of close encounters or even collisions. The particles which undergo such an encounter are likely to be extracted from the resonance. If the planet is massive enough, the FEB generation process should not survive the encounters, all particles being extracted from the resonance before having reached eccentricity large enough to be observed as FEBs. In fact, we tested this hypothesis numerically (results not shown here), with the conclusion that even a Uranus-sized inner planet is able to totally prevent the FEB phenomenon. In such a case however, the inner planet could itself generate FEBs from its own resonances, the first planet acting as a distant perturber. Conversely, if the inner planet is small (say, terrestrial-like) the situation should not dramatically change with respect to the one-planet case, and this situation is investigated in detail in Section 3.

An outer planet has a potentially much weaker disturbing effect, as it always remains for the FEBs a secondary distant perturber. Hence the basic mechanism of FEB generation by mean-motion resonances should survive in that case.

If an outer planet is strong enough to significantly affect the FEB generating mechanism, its mass should be of the same order of magnitude as that of the first planet. If the first planet is comparable to Jupiter, a valuable issue is then to check whether the suspected mechanism is robust toward the presence of an additional Saturn-like planet, located somewhat further away from the star than the main jovian one.

We have simulated the FEB generation process adding an additional planet orbiting the star at $a'' = 20$ AU. with initial eccentricity $e'' = 0.02$. This planet was assumed to be 30% as massive as the first one, in order to mimic the Jupiter–Saturn configuration. The results are illustrated in Fig. 11, which may

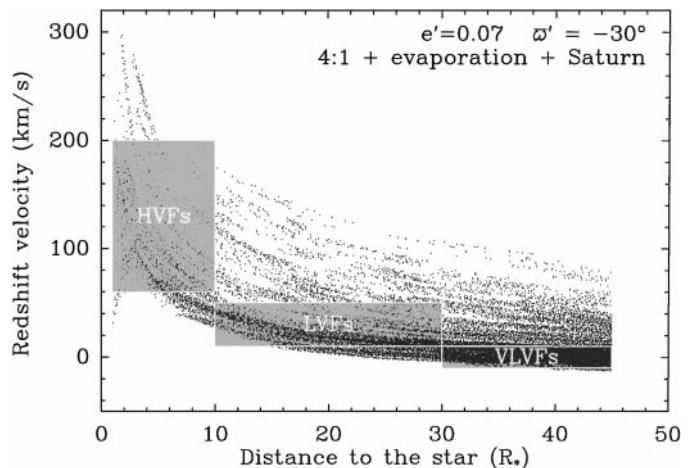


FIG. 11. Same as described in the legend to Fig. 8 (4:1 resonance), but in this case, a Saturn-like planet (30% as massive of the first one), orbiting the star at 20 AU was added. The basic results concerning the FEB phenomenon remain, but the velocity confinement of the events is worse. Note that in order to get a correct fit for the velocities, we must set $\omega' = -30^\circ$ instead of -70° as in Fig. 8.

be directly compared with Fig. 8. The events appear to be somewhat more dispersed on the (stellar distance, redshift velocity) plane than in Fig. 8, so that the present observational data seem to be better fitted by Fig. 8. We stress however that both situations can probably not be distinguished from an observational point of view, taking into account the limited observational temporal coverage of the spectrum of the star. Hence the mechanism appears robust toward the presence of other planets orbiting β Pic, at least orbiting the star at larger distance than the main one.

Recall however that we have not investigated the possible role of secular resonances that are introduced in the planetary system as soon as more than one planet exists. Farinella *et al.* (1994) showed that in the Solar System, the ν_6 secular resonance (involving Saturn) is an active source of Sun-grazing asteroids, and it was suggested by Levison *et al.* (1995) that this could apply to the β Pic case as well, without invoking anything else. However, we have already discussed that this is too far from being generic to be considered as likely.

Much more generic is the case of overlapping mean-motion and secular resonances. This actually occurs in the Solar System's asteroid belt (Morbideilli and Moons 1993, Moons and Morbidelli 1995) and makes the mean-motion resonances much more efficient in pumping the eccentricity of resonant bodies to Sun-grazing values than in the case where only Jupiter exists. We cannot exclude that such a situation applies to the case of β Pic as well, but here it is virtually impossible to explore the whole parameter space. We note however that all studies show that the overlapping of different kinds of resonances tends to strengthen the FEB phenomenon rather than prevent it. In presence of secular resonances, for instance, also the 3:1 resonance and even the 5:2 resonance could become a very active source of FEBs (Morbideilli and Moons 1995), while we showed above that it is only marginally active without additional planets. Activating additional mean-motion resonances is the major effect that an additional outer planet can produce on the FEB phenomenon.

3. INNER TERRESTRIAL-LIKE PLANETS. BLUESHIFTED EVENTS

We now investigate the effect of inner planets on the FEB mechanism. As explained above, the disturbing effect of an inner planet is expected to be much stronger than that of an outer planet, as resonant bodies must cross its orbit before becoming a star-grazer. Moreover, adding a terrestrial-like inner planet may help in understanding the origin of a small family of blueshifted events that has been observed in recent years.

3.1. Blueshifted Events

In a recent paper (Crawford *et al.* 1998), we reported the detection on June 19 and 20, 1997, of a strong transient spectral event in the β Pic spectrum, comparable to the regular LVFs, but *blueshifted* by more than 10 km s^{-1} with respect to the main central component. Revising data we have been gathering for many years, it turned out that these blueshifted events were not the first

of that kind to be observed. In Beust *et al.* (1991), the detection of a \sim zero velocity (blended with the central one) component was reported. In Lagrange-Henri *et al.* (1992), two weak blueshifted components were reported, and similar features are also observed in some (unpublished) data taken in 1996, with blueshifts reaching almost -100 km s^{-1} . Blueshifted components were also marginally identified in Fe II lines with the IUE satellite by Bruhweiler *et al.* (1991). Therefore, the 1997 blueshifted events should just be considered as the strongest ever observed in the β Pic spectrum. Note that they are not the most blueshifted ever observed. The LVF-like blueshifted events appear much less frequently than the redshifted ones. Considering our observational temporal coverage (which is far from being total), a rough frequency estimate leads to ~ 10 blueshifted events per year. This must be compared to the several hundreds of redshifted LVFs that are needed to be compatible with the observations (Beust *et al.* 1996).

Combined with the fact that they are also usually weaker, this is the reason why we did not pay much attention to the blueshifted events until now, considering them as outliers from the main distribution. Such a conclusion no longer appears satisfactory. It seems that a distinct, much less crowded family of FEBs should be considered as responsible for this new observational fact. This new conclusion is dictated by the results of the simulations presented above. In Fig. 8, the blueshifted events should appear as dots in the LVF stellar distance region, but with negative velocities. Now, the lower edge of the dots area in Fig. 8 is very sharp, showing that without any additional perturbation, no outliers toward blueshifted velocities should be expected from such a distribution. Changing the $\varpi' = -70^\circ$ value basically shifts vertically (at least in the LVF domain) the dots area on the plot, but this would shift most of the LVF distribution down to blueshifted values, instead of producing outliers. This is clearly due to the sharp lower edge of the dots area in Fig. 8.

In the frame of the FEB scenario, a blueshifted event is easily obtained from a FEB that is oriented somewhat differently. For a typical LVF-generating body, having a periastron distance of $\sim 20 R_*$, an event in the correct redshifted domain (i.e., $+20$ to $+40 \text{ km s}^{-1}$ with respect to the star) is obtained for a longitude of periastron $\varpi \simeq +20^\circ$ with respect to the line of sight (see simulations in Beust *et al.* 1996). The -14 km s^{-1} component observed on June 19, 1997 (Crawford *et al.* 1998) can be due to a similar body, but with $\varpi \simeq -10^\circ$, i.e., a 30° shift. The output of a the corresponding simulation is shown in Crawford *et al.* (1998).

3.2. A Terrestrial-Like Planet as a Source for the Blueshifted Events

As discussed above, the pure mean-motion resonance model cannot account for the blueshifted events, so that one must look for an additional source, i.e., something to add to the basic model. Additional planets are the only source of perturbations we may add in the disk.

The features of small bodies dynamics in our Solar System suggest that the existence of a terrestrial planet inside the 4:1 resonance location could solve the problem. In fact, the basic idea is the following:

- As the resonant bodies undergo an eccentricity increase, they must cross the orbit of the terrestrial-like planet.
- Because the terrestrial-like planet is not very massive, most of these crossing bodies should not be drastically affected, and should keep evolving inside the 4:1 resonance, becoming “regular,” redshifted FEBs at high eccentricity.
- A *minority* of the bodies are expected to undergo a close encounter with the terrestrial-like planet, causing them to be ejected from the 4:1 resonance with the major planet.
- These bodies are thus extracted from the main FEB generating process, but once extracted, they keep evolving under the perturbations of both planets (essentially the major one), but in a *nonresonant* manner.
- The nonresonant secular evolution causes the eccentricity of these bodies to evolve between an inner and an upper bound. These boundaries are expected to be located at high eccentricity, since the bodies are already at high eccentricity when they are extracted from the resonance. In some cases, the upper bound of this evolution may be high enough to allow those particles to become *nonresonant* observable FEBs.
- The high- e phase of nonresonant bodies occurs for a different periastron orientation than for the resonant bodies, thus explaining why the spectral events associated to nonresonant FEBs are blueshifted. More precisely, we showed in Beust and Morbidelli (1996) that for resonant bodies, the peak eccentricity in the secular evolution (in a planar problem) occurs for $\varpi - \varpi' = 180^\circ$, i.e., with a periastron pointing toward the opposite direction of that of the planet. For nonresonant bodies, the peak occurs for $\varpi = \varpi'$. This may be understood as follows: The secular dynamics is described by the equations of motion after averaging over the short periodic terms. Outside a mean-motion resonance, averaging is done over the mean longitudes λ and λ' of the particle and the planet; inside the 4:1 resonance it must be done over the planet’s mean longitude and along a libration cycle of the resonant angle $4\lambda' - \lambda - 3\varpi$. This leads to different averaged equations, namely to different secular evolutions.

We could also think the blueshifted events family to be generated by the 4:1 resonance of another Jupiter-sized planet located somewhat further away from the star. However, this could work only if the particles trapped into such a resonance do not get too close to the orbit of the first planet; otherwise they would undergo strong perturbations, or even close encounters that would eject them from the resonance. This is fact provides severe constraints. The 4:1 resonance is located at a semi-major axis equal to $\simeq 40\%$ of that of the perturbing planet. During a FEB-like evolution, the semi-major axis of a given resonant particle is not subject to drastic changes, as it only librates around a mean value. As they reach the FEB-regime ($e \simeq 1$), their apoastron is

approximately twice as large as their initial semi-major axis, i.e., $\sim 80\%$ of the semi-major axis of the perturbing planet. The condition that the particles have an apoastron inside the orbit to the first planet allows one to conclude that the second planet should not be located further away from the star than by only $\sim 25\%$ of the orbital distance of the first one. Such a planetary configuration (two giant planets rather close to each other) appears fairly unlikely, as such a system would probably not be dynamically stable, or would have difficulties to form.

The inner terrestrial planet hypothesis seems therefore more likely for our purpose. In our simulations we thus added to the first jovian planet, with $a' = 10$ AU, $e' = 0.07$, an Earth-sized planet orbiting the star at $a'' = 0.8$ AU with zero eccentricity. We also took into account a mutual inclination of 1° as a typical possible value. The only critical point in the choice of the terrestrial planet’s orbital elements is that a'' must be small enough so as to extract bodies from the 4:1 resonance only when they are at very large eccentricity. Only in this case, in fact, may we hope that the extracted bodies evolve to star-grazing eccentricity. Indeed, values of a'' larger than ~ 1 AU turn out not to give satisfactory results.

Because the bodies undergo close encounters, we have used for the simulation the SWIFT_RMVS3 integrator, a modified version of SWIFT written by H. Levison and M. Duncan that takes close encounters into account (Levison and Duncan 1994). We also needed to take a timestep much smaller than that in previous simulations, in order to correctly compute the motion of the terrestrial-like planet.

The result is displayed in Fig. 12. We note that the basic resonant (and redshifted) FEBs are still present, showing that an Earth-sized planet is not powerful enough to extract most of the bodies from the resonance.

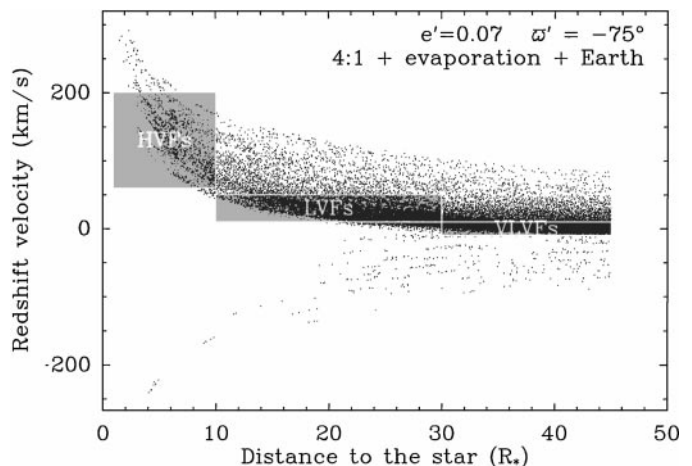


FIG. 12. Same as described in the legend to Fig. 4 (4:1 resonance), but in this case, an Earth-sized planet, orbiting the star at 0.8 AU was added. The basic resonant FEB phenomenon remain, but a few blueshifted nonresonant FEBs are obtained. A better fit is obtained here with $\varpi = -75^\circ$ than with $\varpi = -70^\circ$.

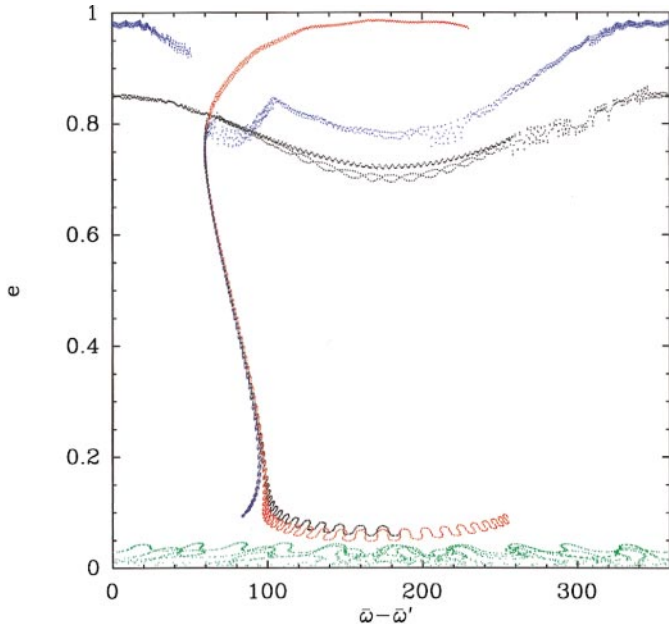


FIG. 13. Evolutionary track of four characteristic particles inside the 4:1 resonance with the jovian planet, once perturbed by the terrestrial-like planet, in a $(\varpi - \varpi', e)$ space.

We also note that a much less crowded family of blueshifted events appears between 0 and -100 km s^{-1} . These correspond to the nonresonant FEBs discussed above, and well simulate the few blueshifted events observed in the β Pic spectrum, in terms of both blueshifted velocity range and frequency.

Finally Fig. 13 illustrates the various dynamical evolutions of four typical particles in the $(\varpi - \varpi', a)$ plane, i.e., in the same space as that used in most of the figures of Beust and Morbidelli (1996). These tracks must then be compared to the analytically computed curves displayed in that paper:

Green track. This particle is trapped in the 4:1 resonance but it is not (yet) subject to any eccentricity increase. As mentioned above, this concerns roughly 50% of the particles, which limits the efficiency of the process.

Red track. This particle evolves inside the resonance from an initially very low eccentricity up to $e \simeq 1$. It does not have any close encounter with the terrestrial-like planet, and thus becomes a “regular” FEB, generating redshifted events;

Black track. This particle is suddenly extracted from the resonance at high eccentricity by a close encounter with the terrestrial-like planet, and thus undergoes a nonresonant dynamical evolution which causes its eccentricity to fluctuate between rather high boundaries, but never in the FEB regime.

Blue track. The same applies to this particle, but its nonresonant dynamics after an encounter with the terrestrial-like planet causes its eccentricity to reach high values to enter the FEB regime, but with a longitude of periastron different than that of the particle corresponding to the red track. This particle becomes a blueshifted events-generating FEB.

4. MASS AND TIME-SCALE RELATED QUESTIONS

4.1. General Features

Most of the unsolved questions concerning the FEB scenario and its implications are related to timescales, roughly at every level of the model.

Concerning the FEB phenomenon itself, the fact that some LVFs seem to last several days long is not straightforwardly explained. At the stellar distances under consideration, the transit time of a FEB across the line of sight indeed does not exceed 6 or 7 h. Consequently, a given component observed two consecutive nights cannot be attributed to the same body, in the framework of our model. This is why we had suggested on the basis of a statistical study that several consecutive passages of different FEBs might account for these observations. Alternatively we could observe chains of bodies moving in the same orbit and passing sequentially in front of the line of sight, much like the recent observations of Comet Shoemaker–Levy 9 in the vicinity of Jupiter. In fact when reaching small periastron values, the FEBs are probably tidally broken up into several individual pieces. In Beust *et al.* (1996), we had shown that a disruption near periastron would cause the fragments to be back at periastron as a chain of comoving bodies.

This hypothesis was also supported by the fact that despite a duration of several days, the LVFs components exhibit variations in their shape within a single night or even less (Lagrange *et al.* 1996), suggesting the successive passage of individual objects. Nevertheless this does not explain the more or less global evolutionary trend detected over a timescale of order of one month (Ferlet *et al.* 1993). Concerning this very point, there is still an obvious lack of data.

As discussed above, the question of the evaporation rate of the bodies is not definitely solved. A more refined analysis is clearly needed and will be carried out in future work. We may however stress that a population consisting of bodies mainly in the radius range 10–20 km or larger is probably much more suited than a population made up exclusively of kilometer-sized bodies, as such small bodies probably do not resist long enough against evaporation.

In Beust and Morbidelli (1996), we also claimed that the time needed for a given body to become an observable FEB ($\sim 10^5$ yr in the present simulations) may appear too short compared to the age of the system. We may however, stress that the situation depicted in the present simulations is very favorable for FEB evolution, as the eccentricity of the jovian planet is fixed at 0.07. In Beust and Morbidelli (1996), we showed that assuming an eccentricity that reaches these values only temporarily, thanks to secular evolution, may cause the typical delay to jump from 10^4 up to $\sim 10^5$ planetary revolutions, i.e., a typical time of a few 10^6 yr. After this time however, the FEB phenomenon should be expected to stop, due to the depletion of the resonance. Now, the age of the star, even if controversial, is estimated to be at least 10^7 yr, and it is more probably closer to 10^8 yr (Paresce 1991, Lanz *et al.* 1995, Brunini and Benvenuto 1996, Crifo *et al.* 1997,

Artymowicz 1997). Hence the FEB phenomenon on β Pic should have ended a long time ago. The mechanism must obviously be replenished at its source. Two possible basic scenarios may be invoked: either new bodies continuously enter the resonance due to mutual collisions and/or gravitational scattering or the resonance sweeps the disk, capturing new bodies.

4.2. Analysis of the Two Proposed Scenarios

4.2.1. Collisions and encounters. There are two possible mechanisms that force changes in the particles' semi-major axis, thus allowing their injection into the resonance: mutual collisions and gravitational scattering due to close encounters with larger bodies. A quantitative analysis of these mechanisms requires a detailed knowledge of the disk's composition (number of particles, size distribution, orbital distribution, bodies' strength, etc.) and is therefore beyond the scope of the present paper. Nevertheless, knowing the number of bodies required to be in the resonance in order to produce the FEB phenomenon and the typical timescale for increasing the eccentricity to stellar-grazing values, it is possible to infer the density of bodies in the disk and the replenishment rate of the resonance, with the following simple argument.

In a steady-stage regime, we can write the conservation of the number of planetesimals per unit time within the resonance as

$$\frac{N_{\text{out}}}{t_{\text{coll}}} = \frac{N_{\text{in}}}{t_{\text{coll}}} + f \frac{N_{\text{in}}}{t_{\text{FEB}}}. \quad (5)$$

In this formula, N_{in} is the linear particle density (number of particles per astronomical unit) that is required in the resonance to produce a large enough number of FEBs (see Section 2.5). Remember that this number takes into account only the bodies larger than some minimal radius r_{min} , because the bodies of smaller size evaporate too quickly to produce observable FEBs (see Section 2.4). Similarly N_{out} is the linear particle density outside of the resonance (still considering only bodies larger than r_{min}). If the resonance did not lose bodies by the FEB phenomenon, N_{in} and N_{out} would be equal. Moreover t_{coll} is the typical time for a particle to suffer a collision/encounter that causes a semi-major axis change larger than the width of the resonance; t_{FEB} is the typical time to increase the eccentricity to ~ 1 inside the resonance (i.e., $\sim 10^5$ yr) and f is the efficiency of the FEB process on resonant particles (roughly 0.4; see above). The left-hand side of this equation accounts for the number of particles that are injected by collisions/encounters into the resonance in the unit of time; on the right-hand side, the first term accounts for particles ejected from the resonance by the same mechanisms and the second term for the particles lost by the FEB process. In Eq. (5) we consider the same typical time t_{coll} for particles both inside and outside the resonance. This is motivated by the fact that the amplitude of the radial motion of the particles during one orbit (namely $2a(e) \simeq 0.4$ AU) is far above the width of the resonance (~ 0.006 AU at $e = 0.1$), so that the resonant particles should mostly encounter nonres-

onant particles along their orbit rather than resonant ones. To be more accurate, one should take into account that the resonant particles that have already reached large eccentricity cross a larger portion of the disk, and move at larger relative velocities with respect to the bodies they collide with. They should therefore have a shorter t_{coll} . The difference however depends on the radial extent of the particles' disk, which is unknown. Moreover, one should not forget that at large eccentricity the resonance is much larger (its width increasing as e^3 , because the 4:1 is a third-order resonance), so that ejection from the resonance becomes more difficult, which in turn increases t_{coll} . The real dependence of t_{coll} on the eccentricity is therefore complicated and cannot be derived by this kind of simple analysis, so that for simplicity we assume t_{coll} to be the same for all bodies.

Equation (5) has solution

$$\frac{N_{\text{out}}}{N_{\text{in}}} = 1 + f \frac{t_{\text{coll}}}{t_{\text{FEB}}}. \quad (6)$$

The computation of N_{out} requires knowing t_{coll} . This is the hard part, because t_{coll} clearly depends on the dominating injection/ejection mechanism and on the disk's composition. Note however that in order to guarantee a large number of FEBs, t_{coll} must be much larger than t_{FEB} ; otherwise most of the resonant bodies would be ejected from the resonance before reaching stellar-grazing values of the eccentricity. Assuming $t_{\text{coll}} = 10t_{\text{FEB}}$ (i.e., 10^6 yr) one gets from (6) $N_{\text{out}} = 5N_{\text{in}}$, namely $10^8 - 10^9$ bodies per astronomical unit. (larger than r_{min}). Such a choice of t_{coll} seems to be compatible with the resulting value of N_{out} ; in fact, 10^6 yr is the mean collision time estimated through a particle in the box computation for a disk of $N = 2 \times 10^8$ particles per astronomical unit at $a = 4$ AU, with mean eccentricity $\langle e \rangle = 0.05$, mean inclination $\langle i \rangle = 0.025$ (in radians) and a radius r of 15 km. This is derived simply writing

$$\frac{1}{t_{\text{coll}}} = \pi r^2 \frac{N}{2\pi a h} v, \quad (7)$$

where h is the thickness of the disk, and v the mean relative velocity of the bodies. We expect to have $h \simeq 2a\langle i \rangle$ and $v \simeq \langle e \rangle v_0$, where $v_0 = \sqrt{GM_*/a}$ is the circular velocity at distance a . With these assumptions, and noting that gravitational scattering is negligible for such velocities and 15-km-radius bodies, we derive the quoted estimate for t_{coll} . In conclusion, we consider that the replenishment of the resonance by the collisional activity in the disk is a plausible mechanism, provided that $N_{\text{out}}/N_{\text{in}} \sim 5$.

4.2.2. Planet migration. It has been recently shown that, during their early history, the planets' orbits are very likely to migrate. This might be due to the scattering of planetesimals (Fernandez and Ip 1984) or by tidal interaction with the disk (Ward 1997, Trilling *et al.* 1998). This kind of mechanism is invoked for accounting for the orbits of the giant extra-solar planet recently discovered in the immediate vicinity of their

parent star (Mayor and Queloz 1995, Butler *et al.* 1997). The location of mean-motion resonances moves together with the migration of the planet, sweeping the small bodies disk. It is well known that if the planet moves toward the central star, the inner mean-motion resonances (the 4:1, for example) capture most of the bodies during the sweeping process. It is reasonable to expect that such a mechanism might be at work today in the β Pic disk, sustaining the FEB phenomenon until the final stabilization of the planetary system. Planet migration in the β Pic system has been recently invoked also by Lecavelier (1998) as a way to force outer bodies trapped in resonances to migrate in eccentricity and release an amount of dust sufficient to preserve the dust disk.

Let us now assume a steady-state situation, where the resonance is continuously refilled by migration and cleared out by the FEB phenomenon. The planet is assumed to migrate at a velocity u , so that the 4:1 resonance migrates at velocity $4^{-2/3}u$. As for the collision model (Eq. 5) we write here the conservation of the number of planetesimals in the resonance per unit time

$$4^{-2/3}N_{\text{out}}u = fN_{\text{in}}\frac{W}{t_{\text{FEB}}}, \quad (8)$$

where W is the width of the resonance, which yields

$$\frac{N_{\text{out}}}{N_{\text{in}}} = 4^{2/3}\frac{fW}{ut_{\text{FEB}}}. \quad (9)$$

In the model by Fernandez and Ip (1984), the migration is caused by ejection of planetesimals by a massive planet. The radial displacement of a protoplanet of mass M_p caused by the ejection of a mass m_e of planetesimals is estimated to

$$\frac{\Delta a}{a} = \exp\left(-2(\sqrt{2}-1)\frac{m_e}{M_p}\right) - 1. \quad (10)$$

According to Fernandez and Ip (1984), the outer planets Uranus and Neptune migrated by several astronomical units during their formation. Now, Jupiter is about 20 times more massive. Hence displacing a Jupiter-sized (or twice as much) planet located at 10 AU by several astronomical units would require ejecting a mass or planetesimals comparable to the mass of Jupiter. This may appear more difficult. As a matter of fact, the radial displacement of Jupiter in the early Solar System is estimated to be only 0.2 AU (Liou and Malhotra 1997).

If we thus assume a migration rate of 0.2 AU in 10^8 yr, we get $N_{\text{out}}/N_{\text{in}} \simeq 30$, which is significantly above what was deduced in the previous section. In fact, the migration rate assumed here is so small that a large overdensity outside the resonance is required in order to bring into the resonance a sufficient number of bodies. In other words, the resonance must be strongly depleted with respect to the rest of the disk.

The model based on the tidal interaction with a protoplanetary disk described by Ward (1997) and Trilling *et al.* (1998) seems to produce more important migrations, and could appear

better suited to the present case. Ward (1997) distinguished two kinds of migrations (types I and II), and gave the corresponding rates

$$u_{\text{I}} \sim c_1 \left(\frac{M_p}{M_*}\right) \left(\frac{\sigma r^2}{M_*}\right) \left(\frac{v_0}{c}\right)^3 v_0; \quad (11)$$

$$u_{\text{II}} \sim c_2 \alpha \left(\frac{c}{v_0}\right)^2 v_0, \quad (12)$$

where c is the gas sound speed, and σ is the surface density of the disk, c_1 and c_2 are coefficients of order unity and α is typically 10^{-3} or 10^{-4} . If we assume a temperature of 150 K and a typical, linear mass density of $1 M_{\oplus}$ per astronomical unit, both velocities appear to be $10^{-6}v_0$ or $10^{-5}v_0$, and we get $N_{\text{out}}/N_{\text{in}}$ values ranging between 10^{-3} and 10^{-2} , showing that now there is a high overdensity in the resonance. The resonance is moving so fast that the resonance is refilled quicker than it is cleared out. We believe nevertheless that the present description is erroneous in that case.

First, invoking the tidal interaction with a gas disk supposes that a massive enough disk exists. In fact there is actually some gas in the β Pic system, which is seen as the central stable circumstellar component permanently seen in the spectral lines of β Pic next to the FEB variable ones. In Lagrange *et al.* (1998), it was shown that such a disk could be sustained by the FEB activity or a weak stellar wind, provided there is some volatile material somewhere in the disk to stop the gaseous metallic ions. This amount of gas is nevertheless small and may be unable to generate any tidal interaction. Moreover, its location within the disk is very poorly constrained. Hence the relevance of the Ward (1997) and Trilling *et al.* (1998) model for the β Pic case remains questionable.

Second, when the resonance is moving very fast, the efficiency of the resonant trapping drops, so that it is not sure whether the refilling mechanism is that active. Moreover, the dynamical evolution of the resonant, particles could be affected by the motion of the resonance, perhaps cutting off the FEB phenomenon, or enhancing it. The integrations we present here would then not apply to this case. Obviously a dedicated study must be carried out in order to investigate this issue. This will be the subject of future work.

Note finally that if the motion of mean-motion resonances is severely constrained by the semi-major axis migration of the planet, the eventual secular resonances in the planetary system may move much more drastically during the same time. The total migration of the ν_{16} and ν_6 resonances in the early Solar System history is estimated to be ~ 1 AU (Gomes 1997). Hence secular resonances, although probably not able to generate the FEB phenomenon themselves, may help (i) activate some of the mean-motion resonances (3:1 or 5:2) and make them sources of FEBs and (ii) excite the whole disk by a rapid sweeping, throwing fresh bodies into the mean-motion resonances. This point should be investigated in future work.

4.3. Disk Mass Estimates

In Section 2.5 we estimated that inside the resonance, the linear density of bodies N_{in} should range between 2×10^7 and 2×10^8 bodies per astronomical unit. In the previous section, different models for refilling the resonance allowed us to derive estimates for the density outside the resonance N_{out} . Recall that these densities are computed for bodies larger than a minimal value r_{min} (~ 15 km). It is now of valuable interest to translate this into a mass estimate. The linear mass density is given by

$$M_1 = \int_0^{r_{\text{max}}} N_{\text{out}} p(r) \frac{4}{3} \pi \rho r^3 dr, \quad (13)$$

where $p(r)$ is the size distribution introduced in (4), that is normalized for the bodies larger than r_{min} (because N_{out} stands for the linear density of bodies larger than this size), and ρ the mass density of the bodies.

In the integral (13), the size distribution has been arbitrarily truncated to some maximum size r_{max} to avoid divergence. In fact, with the $r^{-3.5}$ size distribution, all the mass is concentrated into the largest bodies.

In the asteroid belt the $r^{-3.5}$ size distribution is no longer valid for asteroids larger than ~ 30 km (Durda *et al.* 1998). This size distribution arises from self-similar collision equilibrium at all sizes (Dohnanyi 1969). The largest bodies have significant gravity so that their collisional regime is affected. In the more crowded system of β Pic, we expect the collisional regime to extend somewhat beyond this limit, as the disk is more collisionally active. For the same reason, the simulations of Durda *et al.* (1998) assumed that the size distribution within the *primordial* asteroid belt followed the $r^{-3.5}$ law up to bodies as large as several hundreds of kilometers. Thus, we decide to assume for r_{max} the size of the largest solar asteroid, Ceres, i.e., $r_{\text{max}} = 500$ km. The mass estimates we derive below should then be considered valid for bodies up to Ceres-sized. It is plausible, however, that larger bodies exist in the disk (possibly of size comparable to that of the terrestrial planets), the total mass in the β Pic system being higher by an unconstrained factor.

From (13), the linear mass density carried by bodies smaller than r_{max} results in

$$M_1 = \frac{20}{3} \pi N_{\text{out}} r_{\text{min}}^3 \rho \left(\sqrt{\frac{r_{\text{max}}}{r_{\text{min}}}} - 1 \right). \quad (14)$$

Note that this estimate has a strong dependence on r_{min} , whose value is very model dependent. Small changes of the latter would introduce large changes in the total mass estimate. Recall that r_{min} was deduced from an estimate of the evaporation rate of the FEBs when crossing the line of sight. This estimate is model-dependent (see Beust *et al.* 1996), and should be considered as accurate within one order of magnitude only. With $r_{\text{max}} =$

500 km, $r_{\text{min}} = 15$ km, and $\rho = 1 \text{ g cm}^{-3}$, (14) becomes

$$M_{r \leq r_{\text{max}}} \simeq 6.8 M_{\oplus} \times \frac{N_{\text{out}}}{10^8 \text{ AU}^{-1}}. \quad (15)$$

In the collisional refilling model, we estimate N_{out} between 10^8 and 10^9 AU^{-1} , which leads to a mass estimate between 6.8 and $68 M_{\oplus}$ per astronomical unit.

Assuming now the refilling by planet migration due to planetesimal scattering, we derive N_{out} values between 6×10^8 and 6×10^9 per astronomical unit or $M_{r \leq r_{\text{max}}}$ ranging now between 45 and $450 M_{\oplus}$ per astronomical unit.

Conversely, if we consider now the planet migration velocities of Ward (1997), N_{out} ranges now between 2×10^4 and $2 \times 10^6 \text{ AU}^{-1}$, and the corresponding $M_{r \leq r_{\text{max}}}$ between 1.5×10^{-3} and $0.15 M_{\oplus} \text{ AU}^{-1}$, which is now more reasonable. Recall however from the previous section that this model is questionable from the point of view of (i) the presence of a massive gaseous disk able to generate tidal interaction, (ii) the efficiency of the process of capture into resonance, and (iii) of that of eccentricity pumping within the resonance.

What should these estimates be compared to? The β Pic system is thought to be much younger than the Solar System, so that the comparison should be done with the surface density of solid material in the primitive Solar System, more specifically with the primordial asteroid belt. The present mass of the asteroid belt is very low ($\sim 5 \times 10^{-4} M_{\oplus}$ for a width of ~ 1 AU), but comparison with the surface density outside the main belt leads one to think that most of the primordial mass within the belt was lost. Rescaling the asteroid value to the $r^{-3/2}$ power law that seems to apply in the rest of the Solar System yields a ‘‘primordial’’ mass density of $\sim 40 \text{ g cm}^{-2}$, i.e., $\sim 9.5 M_{\oplus}$ per astronomical unit (Weidenschilling 1977). This mass estimate falls at the low end of the range deduced from the collision model. We recall however that our mass estimate does not take into account the contribution of the bodies larger than 500 km, while the Weidenschilling (1977) estimate should concern the entire mass. Now, the mass estimate that we obtain from the model of planet migration due to planetesimal scattering seems to be completely unrealistic.

Conversely, the estimate deduced from the migration model by Ward (1997) seems more realistic, but the model itself in the contest of the β Pic system is questionable.

Another important issue is the amount of mass evaporated by the FEB process over the age of the system. Taking our estimate for N_{in} (which does not depend on the refilling model that we assume), the total mass within the 4:1 resonance at $e \leq 0.1$ (width 0.006 AU) falls within the range (still assuming the same size distribution and truncating at $r_{\text{max}} = 500$ km)

$$9.0 \times 10^{-3} \lesssim M_{4:1} \lesssim 9.0 \times 10^{-2} M_{\oplus}. \quad (16)$$

The characteristic time for a given particle to become a FEB is $\sim 10^5$ yr. This should also correspond to the characteristic

clearing time of the resonance. We should then expect all the mass located within the resonance to be consumed by the FEB process within that time. We noted however in our integrations that the efficiency of the FEB mechanism among a given population located within the resonance is only $\sim 40\%$ (the factor f assumed above). Hence only 40% of the mass quoted above should be consumed within 10^5 yr. The FEB process is also possibly not permanently active. As explained in Beust and Morbidelli (1996), it is efficient only if the eccentricity of the perturbing planet e' is larger than ~ 0.05 . The present simulations have been performed assuming $e' = 0.07$. In Beust and Morbidelli (1996), we claimed that e' possibly undergoes secular oscillations between a minimum and a maximum value, over a typical period of a few 10^5 yr, as is the case with Jupiter in our Solar System. These eccentricity oscillations would not completely inhibit the FEB phenomenon: as shown in Beust and Morbidelli (1996) and confirmed by the simulation in Section 2.7 that includes the effects of an additional Saturn-like planet, the FEB phenomenon is activated roughly during the period that $e' > 0.05$. Then, considering a typical case where the planetary eccentricity has a sinusoidal oscillation between $e' = 0$ and $e' = 0.1$, we would expect that the FEB process is active half of the time. In this case, we would just be lucky (at a 50% level) to witness an active phase today. If the maximum eccentricity is smaller than 0.1, the FEB process should be less frequently active; if it were too rarely active, the chance to observe it at the present time would be small. Hence we may consider as reasonable a FEB activity during 50% of the time over the age of the system. Assuming a clearing-out time of $\sim 10^5$ yr during activity, the resonance should have been refilled ~ 500 times since the formation of the star ($\sim 10^8$ yr ago). At each of these times, $\sim 40\%$ of $M_{4:1}$ is consumed by the FEB process. Therefore the total mass consumed by the FEB process over 10^8 yr results in

$$1.8 M_{\oplus} \lesssim M_{\text{consumed}} \lesssim 18 M_{\oplus}. \quad (17)$$

These values are comparable to the mass existing in the disk in a 1 AU range, according to our estimates based on the collisional model for resonance replenishment. This would imply that the FEB phenomenon has been able to remove a significant fraction of the mass of the primordial planetesimal disk. A similar situation has probably occurred in the primordial asteroid belt during the early ages of the Solar System.

4.4. Collective Effects

According to the collisions model, the frequency of the FEB phenomenon seems therefore to require the planetesimal disk mass density to be typically $\sim 10 M_{\oplus}$ per astronomical unit. This amount of mass is far from being negligible. It is then of valuable interest to investigate whether self-gravity effects may affect the dynamics of the particles trapped within the resonance, in particular inhibiting the secular increase of the eccentricity up to stellar-grazing values. Collective effects were of course not been taken into account in the simulations described here,

as the FEBs were treated as negligible mass test particles. The question of the collective particle behavior of a planetesimal disk near mean-motion resonances with a perturbing planet was analytically investigated by Hahn *et al.* (1995), although this study was limited to Lindblad resonances, which for nearly Keplerian disks correspond to first-order mean-motion resonances ($m : (m \pm 1)$), which is not the case here (4:1). Their basic conclusions should however at least qualitatively hold for higher order resonances.

According to their analysis, the main length scale of the collective response is $r\sqrt{2\epsilon}$, where

$$\epsilon = \frac{2\pi G\sigma}{3mr\Omega^2} = \frac{rM_1}{3mM_*}, \quad (18)$$

where M_* is the mass of the star, r is the distance to the star, σ is the mass density of the disk ($M_1 = 2\pi r\sigma$), and Ω is the circular angular velocity at distance r (related to M_* by Kepler's third law). Numerically, with $M_1 \sim 10 M_{\oplus}$ AU, we get $\epsilon = 2.3 \times 10^{-5}/m$, and $r\sqrt{2\epsilon} \simeq 2.7 \times 10^{-2}/\sqrt{m}$ AU. Collective effects are expected to occur provided the length scale exceeds both (i) the characteristic spacing among the bodies, which is typically $\sqrt{m_{\text{particle}}}/\sigma$, and (ii) the radial excursions of the particles in the disk, i.e., $2a(e)$ (Ward and Hahn 1998). Condition (i) is easily fulfilled. In fact, assuming a typical planetesimal to have a 15-km radius, we obtain a spacing of 5.2×10^{-4} AU, which is smaller than $r\sqrt{2\epsilon}$. Condition (ii) implies that the typical eccentricity of the particles in the disk should be smaller than 0.0034. This threshold value is unrealistically small. The existence of the FEB phenomenon implies that the mean eccentricity of the particles in the disk is of order 0.05, i.e., 15 times larger. We therefore conclude that the disk is too dynamically excited to carry density waves, so that collective effects can be completely neglected.

5. CONCLUSIONS

In this paper, we have numerically investigated the dynamics of particles in mean-motion resonances with a jovian-like planet, as a potential source for the FEB phenomenon. The main results are the following:

- The 4:1 mean-motion resonance is a very efficient source for FEBs. The dynamical properties of the simulated FEBs match fairly well those deduced from previous observations and related modeling. Moreover, the mechanism appears robust toward the presence of additional outer planets within the β Pic system.
- A population made of bodies larger than 10 km seems better suited to produce FEBs, than kilometer-sized bodies which should evaporate too quickly.
- The rare blueshifted events recently identified may be explained by the presence of a terrestrial-like planet orbiting the star inside the 4:1 resonance location. More data and statistics about these blueshifted events are clearly needed in order to be

more quantitative in the comparison between observations and simulations.

- The puzzling persistence of the FEB phenomenon at the present age of the star may be explained in a scenario which accounts for the collisional injection of new bodies into the 4:1 resonance.

Unfortunately, our model on the origin of FEBs implies the existence of a too massive planetesimal disk in the β Pic system (from one to several tens of earth masses per astronomic unit). This seems to be a weakness of the model. We do not believe, however, that this is enough to reject the model in its globality. As with most models, ours probably oversimplifies the reality. In addition, several parameters are badly constrained, so that the final mass estimate could be possibly wrong (in either direction) by an order of magnitude, if not more. To obtain more quantitative estimates, it would be necessary to perform a global simulation, taking into account both the dynamics and the effects of close encounters and collisions, but this goes beyond the purpose of the present paper.

We stress, moreover, that no other model on the origin of FEBs around β Pic has ever been investigated in details comparable to those discussed in the present paper.

ACKNOWLEDGMENTS

We warmly thank Dr. P. Thébaud for valuable discussions concerning collision models. All the computations presented in this paper were performed at the “Service Commun de Calcul Intensif de l’Observatoire de Grenoble (SCCI).”

REFERENCES

- Artymowicz, P. 1997. β Pictoris: An early Solar System? *Annu. Rev. Earth Planet. Sci.* **25**, 175–219.
- Bailey, M. E., J. E. Chambers, and G. Hahn 1992. Origin of star-grazers: A frequent cometary endstate. *Astron. Astrophys.* **257**, 315–322.
- Beust, H., and A. Morbidelli 1996. Mean-motion resonances as a source for infalling comets toward β Pictoris. *Icarus* **120**, 358–370.
- Beust, H., A.-M. Lagrange, I. A. Crawford, C. Goudard, J. Spyromilio, and A. Vidal-Madjar 1998. The β Pictoris circumstellar disk. XXV. The Ca II absorption lines and the falling evaporating bodies model revisited using UHRF observations. *Astron. Astrophys.* **338**, 1015–1030.
- Beust, H., A.-M. Lagrange, F. Plazy, and D. Mouillet 1996. The β Pictoris circumstellar disk. XXII. Investigating the model of multiple cometary infalls. *Astron. Astrophys.* **310**, 181–198.
- Beust, H., A.-M. Lagrange-Henri, A. Vidal-Madjar, and R. Ferlet 1990. Numerical simulations of infalling evaporating bodies. *Astron. Astrophys.* **236**, 202–216.
- Beust, H., A. Vidal-Madjar, R. Ferlet, A.-M. Lagrange-Henri 1991. The β Pictoris circumstellar disk. XI. New Ca II absorption features reproduced numerically. *Astron. Astrophys.* **241**, 488–492.
- Boggess, A., F. C. Bruhweiler, C. A. Grady, D. C. Ebbets, Y. Kondo, L. M. Trafton, J. C. Brandt, and S. R. Heap 1991. First results from the Goddard high-resolution spectrograph: Resolved velocity and density structures in the β Pictoris circumstellar disk. *Astrophys. J.* **377**, L49–L52.
- Brahic, A. 1977. Systems of colliding bodies in a gravitational field. I. Numerical simulation of the standard model. *Astron. Astrophys.* **54**, 895–907.
- Bruhweiler, F. C., Y. Kondo, and C. A. Grady 1991. Mass outflow in the nearby protoplanetary system. β Pictoris. *Astrophys. J.* **371**, L27–L31.
- Brunini, A., and O. Benvenuto 1996. β Pictoris: Its evolutionary status. *Mon. Not. R. Astron. Soc.* **283**, L84–L88.
- Burrows, C., J. E. Krist, and K. R. Stapelfeldt 1995. HST observations of the β Pictoris circumstellar disk. *Bull. Am. Astron. Soc.* **187**, Abs. 32.05.
- Butler, R. P., and G. W. Marcy 1996. A planet orbiting 47 Ursae Majoris. *Astrophys. J.* **464**, L153–L156.
- Butler, R. P., G. Marcy, E. Williams, H. Hauser, and P. Shirts 1997. Three new “51 Pegasi-type” planets. *Astrophys. J.* **474**, L115–L118.
- Cheng, K.-P., F. C. Bruhweiler, and J. E. Neff 1997. Detection of β Pictoris-like gaseous infall in 2 Andromedae. *Astrophys. J.* **481**, 866–871.
- Crawford, I. A., H. Beust, and A.-M. Lagrange 1998. Detection of a strong transient blueshifted absorption component in the β Pictoris disc. *Mon. Not. R. Astron. Soc.* **294**, L31–L34.
- Crifo, F., A. Vidal-Madjar, R. Lallemand, R. Ferlet, and M. Gerbaldi 1997. β Pictoris revisited by Hipparcos. Star properties. *Astron. Astrophys.* **320**, L29–L32.
- Dohnanyi, J. S. 1969. Collisional model of asteroids and their debris. *J. Geophys. Res.* **74**, 2531–2554.
- Durda, D. D., R. Greenberg, and R. Jedicke 1998. Collisional models and scaling laws: A new interpretation of the shape of the main-belt asteroid size distribution. *Icarus* **135**, 431–440.
- Farinella, P., Ch. Froeschlé, C. Froeschlé, R. Gonczi, G. Hahn, A. Morbidelli, and G. B. Valsecchi 1994. Asteroids falling onto the Sun. *Nature* **371**, 315–317.
- Ferlet, R., A.-M. Lagrange-Henri, H. Beust, R. Vitry, J. P. Zimmermann, J.-P. Martin, S. Char, M. Belmahdi, J.-P. Clavier, P. Coupiac, B. H. Foing, F. Sevre, and A. Vidal-Madjar 1993. The β Pictoris protoplanetary system. XIV. Simultaneous observations of the Ca II H and K lines; evidence for diffuse and broad absorption features. *Astron. Astrophys.* **267**, 137–144.
- Fernandez, J. A., and W.-H. Ip 1984. Some dynamical aspects of the accretion of Uranus and Neptune—The exchange of orbital angular momentum with planetesimals. *Icarus* **58**, 109–120.
- Festou, M. C., H. Rickman, and R. M. West 1993. Comets. II. Models, evolution, origin and outlook. *Astron. Astrophys. Rev.* **5**, 37–163.
- Flammer, K. R., D. A. Mendis, and H. L. F. Houppis 1998. On the outgassing profile of Comet Hale-Bopp. *Astrophys. J.* **494**, 822–827.
- Gomes, R. S. 1997. Dynamical effects of planetary migration on the primordial asteroid belt. *Astron. J.* **114**, 396–401.
- Grady, C. A., M. R. Pérez, A. Talavera, K. S. Bjorkman, D. De Winter, P. S. Thé, F. J. Molster, M. E. van den Ancker, M. L. Sitko, N. D. Morrison, M. L. Beaver, B. McCollum, and M. W. Castelaz 1996. The β Pictoris phenomenon among Herbig Ae/Be stars. UV and optical high dispersion spectra. *Astron. Astrophys. Suppl. Ser.* **120**, 157–177.
- Grady, C. A., M. L. Sitko, K. S. Bjorkman, M. R. Pérez, D. K. Lynch, R. W. Russell, and M. S. Hanner 1997. The star-grazing extrasolar comets in the HD 100546 system. *Astrophys. J.* **483**, 449–456.
- Greenberg, J. M. 1998. Making a comet nucleus. *Astron. Astrophys.* **330**, 375–380.
- Grinin, V. P., A. Natta, and L. Tambovtseva 1996. Evaporation of star-grazing bodies in the vicinity of UX Ori-type stars. *Astron. Astrophys.* **313**, 857–865.
- Grinin, V. P., P. S. Thé, D. De Winter, M. Giampapa, A. N. Rostopchina, L. V. Tambovtseva, and M. E. van den Ancker 1994. The β Pictoris phenomenon among young stars. I. The case of the Herbig Ae star UX Orionis. *Astron. Astrophys.* **292**, 165–174.
- Hahn, J. M., W. R. Ward, and T. W. Rettig 1995. Resonant trapping in a self-gravitating planetesimal disk. *Icarus* **117**, 24–44.
- Kalas, P., and D. Jewitt 1995. Asymmetries in the β Pictoris dust disk. *Astron. J.* **110**, 794–804.
- Kondo, Y., and F. C. Bruhweiler 1985. IUE observations of β Pictoris: An IRAS candidate for a protoplanetary system. *Astrophys. J.* **291**, L1–L5.

- Lagrange, A.-M., H. Beust, D. Mouillet, M. Deleuil, P. D. Feldman, R. Ferlet, L. Hobbs, A. Lecavelier Des Etangs, J. J. Lissauer, M. A. McGrath, J. B. McPhate, J. Spyromilio, W. Tobin, and A. Vidal-Madjar 1998. The β Pictoris circumstellar disk. XXIV. Clues to the origin of the stable gas. *Astron. Astrophys.* **330**, 1091–1108.
- Lagrange, A.-M., F. Plazy, H. Beust, D. Mouillet, M. Deleuil, R. Ferlet, J. Spyromilio, A. Vidal-Madjar, W. Tobin, J. B. Hearnshaw, M. Clark, and K. W. Thomas 1996. The β Pictoris circumstellar disk. XXI. Results of the December 1992 spectroscopic campaign. *Astron. Astrophys.* **310**, 547–563.
- Lagrange-Henri, A.-M., H. Beust, R. Ferlet, and A. Vidal-Madjar 1989. The β Pictoris circumstellar disk. VIII. Evidence for a clumpy structure of the infalling gas. *Astron. Astrophys.* **215**, L5–L8.
- Lagrange-Henri, A.-M., E. Gosset, H. Beust, R. Ferlet, and A. Vidal-Madjar 1992. The β Pictoris circumstellar disk. XIII. Survey of the variable Ca II lines. *Astron. Astrophys.* **264**, 637–653.
- Lagrange-Henri, A.-M., A. Vidal-Madjar, and R. Ferlet 1988. The β Pictoris circumstellar disk. VI. Evidence for material falling onto the star. *Astron. Astrophys.* **190**, 275–282.
- Lamers, H. J. G. L. M., A. Lecavelier des Etangs, and A. Vidal-Madjar 1997. β Pictoris light variations. II. Scattering by a dust cloud. *Astron. Astrophys.* **328**, 321–330.
- Lanz, T., S. R. Heap, and I. Hubeny 1995. HST/GHRS observations of the β Pictoris system: Basic parameters of the age of the system. *Astrophys. J.* **447**, L41–L44.
- Lazzaro, D., B. Sicardy, F. Roques, and R. Greenberg 1994. Is there a planet around β Pictoris? Perturbations of a planet on a circumstellar dust disk. 2. The analytical model. *Icarus* **108**, 59–80.
- Lecavelier des Etangs, A. 1998. Planetary migration and sources of dust in the β Pictoris disk. *Astron. Astrophys.* **337**, 501–511.
- Lecavelier des Etangs, A., M. Deleuil, A. Vidal-Madjar, R. Ferlet, C. Nitschelm, B. Nicolet, and A.-M. Lagrange-Henri 1995. β Pictoris. Evidence for light variations. *Astron. Astrophys.* **299**, 557–562.
- Lecavelier des Etangs, A., M. Deleuil, A. Vidal-Madjar, A.-M. Lagrange-Henri, D. Backman, J. J. Lissauer, R. Ferlet, H. Beust, and D. Mouillet 1997b. HST-GHRS observations of candidate β Pictoris-like circumstellar gaseous disks. *Astron. Astrophys.* **325**, 228–236.
- Lecavelier des Etangs, A., A. Vidal-Madjar, G. Burki, H. J. G. L. M. Lamers, R. Ferlet, C. Nitschelm, and F. Sèvre 1997a. β Pictoris light variations. I. The planetary hypothesis. *Astron. Astrophys.* **328**, 311–320.
- Lecavelier des Etangs, A., A. Vidal-Madjar, and R. Ferlet 1996. Dust distribution in disks supplied by small bodies: Is the β Pictoris disk a gigantic multi-cometary tail? *Astron. Astrophys.* **307**, 542–550.
- Levison, H. F., and M. J. Duncan 1994. The long-term dynamical behavior of short-period comets. *Icarus* **108**, 18–36.
- Levison, H. F., M. J. Duncan, and G. W. Wetherill 1995. Secular resonances and cometary orbits in the β Pictoris system. *Nature* **372**, 441–444.
- Liou, J.-C., and R. Malhotra 1997. Depletion of the outer asteroid belt. *Science* **275**, 375–377.
- Lissauer, J. J. 1993. Planet formation. *Ann. Rev. Astron. Astrophys.* **31**, 129–174.
- Marcy, G. W., and R. P. Butler 1996. A planetary companion to 70 Virginis. *Astrophys. J.* **464**, L147–L151.
- Mayor, M., and D. Queloz 1995. A Jupiter-mass companion to a solar-type star. *Nature* **378**, 355–359.
- Moons, M., and A. Morbidelli 1995. Secular resonances inside mean-motion commensurabilities. The 4/1, 3/1, 5/2, and 7/3 cases. *Icarus* **114**, 33–50.
- Morbidelli, A., and M. Moons 1993. Secular resonances in mean motion commensurabilities—The 2/1 and 3/2 cases. *Icarus* **102**, 316–332.
- Morbidelli, A., and M. Moons 1995. Numerical evidence on the chaotic nature of the 3/1 mean motion commensurability. *Icarus* **115**, 60–65.
- Mouillet, D., J. D. Larwood, J. C. B. Papaloizou, and A.-M. Lagrange 1997. A planet on an inclined orbit as an explanation of the warp in the β Pictoris disc. *Mon. Not. R. Astron. Soc.* **292**, 896–904.
- Paresce, F. 1991. On the evolutionary status of β Pictoris. *Astron. Astrophys.* **247**, L25–L27.
- Rickman, H. 1992. Physico-dynamical evolution of aging comets. In *Interrelations between Physics and Dynamics for Minor Bodies in the Solar System* (D. Benest and C. Froeschlé, Eds.), pp. 197–263. Editions Frontières, Gij-sur-Yvette.
- Roques, F., H. Scholl, B. Sicardy, and B. Smith 1994. Is there a planet around β Pictoris? Perturbations of a planet on a circumstellar disk. 1. The numerical model. *Icarus* **108**, 37–58.
- Sekanina, Z. 1991. Cometary activity, discrete outgassing areas, and dust-jet formation. In *Comets in the Post-Halley Era* (R. L. Newburn, Jr., M. Neugebauer, and J. Rahe, Eds.), pp. 769–823. Kluwer Academic, Dordrecht.
- Smith, B., and R. Terrile 1984. A circumstellar disk around β Pictoris. *Science* **226**, 1421–1424.
- Trilling, D. E., W. Benz, T. Guillot, J. I. Lunine, W. B. Hubbard, and A. Burrows 1998. Orbital evolution and migration of giant planets: Modeling extrasolar planets. *Astrophys. J.* **500**, 428–439.
- Vidal-Madjar, A., L. M. Hobbs, R. Ferlet, C. Gry, and C. E. Albert 1986. The circumstellar gas cloud around β Pictoris. II. *Astron. Astrophys.* **167**, 325–332.
- Vidal-Madjar, A., A.-M. Lagrange-Henri, P. D. Feldman, H. Beust, J. J. Lissauer, M. Deleuil, R. Ferlet, C. Gry, L. M. Hobbs, M. A. McGrath, J. B. McPhate, and H. W. Moos 1994. HST-GHRS observations of β Pictoris: Additional evidence for infalling comets. *Astron. Astrophys.* **290**, 245–258.
- Vidal-Madjar, A., A. Lecavelier des Etangs, and R. Ferlet 1998. β Pictoris, a young planetary system? A review. *Planet. Space Sci.* **46**, 629–648.
- Ward, W. R. 1997. Survival of planetary systems. *Astrophys. J.* **482**, L211–L214.
- Ward, W. R., and J. M. Hahn 1998. Dynamics of the trans-Neptune region: Apical waves in the Kuiper belt. *Astron. J.* **116**, 489–498.
- Weidenschilling, S. J. 1977. The distribution of mass in the planetary system and solar nebula. *Astrophys. Space Sci.* **51**, 153–158.